

RL-TR-97-52
In-House Report
August 1997



THEORIES AND APPROACHES TO ELECTROMAGNETIC TRANSMISSION IN NON-ISOTROPIC MATERIALS

Dawn Cryer

19971007 221

APPROVED FOR PUBLIC RELEASE; DISTRIBUTION UNLIMITED.

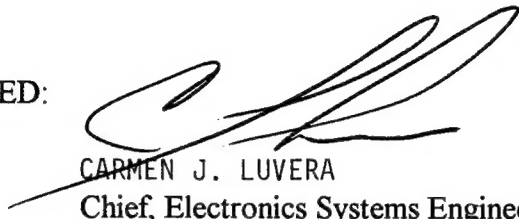
DTIC QUALITY INSPECTED 4

**Rome Laboratory
Air Force Materiel Command
Rome, New York**

This report has been reviewed by the Rome Laboratory Public Affairs Office (PA) and is releasable to the National Technical Information Service (NTIS). At NTIS it will be releasable to the general public, including foreign nations.


RL-TR-97-52 has been reviewed and is approved for publication.

APPROVED:



CARMEN J. LUVERA
Chief, Electronics Systems Engineering Division
Electromagnetics & Reliability Directorate

FOR THE DIRECTOR:



JOHN J. BART, Chief Scientist
Reliability Sciences

If your address has changed or if you wish to be removed from the Rome Laboratory mailing list, or if the addressee is no longer employed by your organization, please notify Rome Laboratory/ERST, Rome, NY 13441. This will assist us in maintaining a current mailing list.

Do not return copies of this report unless contractual obligations or notices on a specific document require that it be returned.

REPORT DOCUMENTATION PAGE			Form Approved OMB No. 0704-0188	
Public reporting burden for this collection of information is estimated to average 1 hour per response, including the time for reviewing instructions, searching existing data sources, gathering and maintaining the data needed, and completing and reviewing the collection of information. Send comments regarding this burden estimate or any other aspect of this collection of information, including suggestions for reducing this burden, to Washington Headquarters Services, Directorate for Information Operations and Reports, 1215 Jefferson Davis Highway, Suite 1204, Arlington, VA 22202-4302, and to the Office of Management and Budget, Paperwork Reduction Project (0704-0188), Washington, DC 20503.				
1. AGENCY USE ONLY (Leave blank)		2. REPORT DATE August 1997		3. REPORT TYPE AND DATES COVERED In-House
4. TITLE AND SUBTITLE THEORIES AND APPROACHES TO ELECTROMAGNETIC TRANSMISSION IN NON-ISOTROPIC MATERIALS			5. FUNDING NUMBERS PE - 62702F PR - 2338 TA - 03 WU-1Q	
6. AUTHOR(S) Dawn Cryer				
7. PERFORMING ORGANIZATION NAME(S) AND ADDRESS(ES) Rome Laboratory/ERST 525 Brooks Road Rome, NY 13441-4505			8. PERFORMING ORGANIZATION REPORT NUMBER RL-TR-97-52	
9. SPONSORING/MONITORING AGENCY NAME(S) AND ADDRESS(ES) Rome Laboratory/ERST 525 Brooks Road Rome, NY 13441-4505			10. SPONSORING/MONITORING AGENCY REPORT NUMBER RL-TR-97-52	
11. SUPPLEMENTARY NOTES Rome Laboratory Project Engineer: David O. Ross/ERST/(315)330-7624				
12a. DISTRIBUTION AVAILABILITY STATEMENT Approved for public release; distribution unlimited.			12b. DISTRIBUTION CODE	
13. ABSTRACT (Maximum 200 words) Advanced composite materials are used extensively for commercial and military aircraft applications. This paper reviews numerous approaches and theories used for evaluating electromagnetic transmission through a variety of composite materials classes. The types of composite materials discussed are 1) graphite/epoxy composites; 2) chiral composites; 3) omega particulate composites; 4) quasioptic composites; and 5) dielectric composites. Due to the availability of open literature references, the primary focus is constrained of the first two classes (graphite/epoxy and chiral composites). Topics discussed include AC circuit simulation programs, phase-correction modeling, and wave propagation theory.				
14. SUBJECT TERMS EM interactions, Em theory, composite materials			15. NUMBER OF PAGES 48	
			16. PRICE CODE	
17. SECURITY CLASSIFICATION OF REPORT UNCLASSIFIED	18. SECURITY CLASSIFICATION OF THIS PAGE UNCLASSIFIED	19. SECURITY CLASSIFICATION OF ABSTRACT UNCLASSIFIED	20. LIMITATION OF ABSTRACT UL	

ABSTRACT

Advanced composite materials are used extensively for commercial and military aircraft applications. This paper reviews numerous approaches and theories used for evaluating electromagnetic transmission through a variety of composite materials classes. The types of composite materials discussed are: 1) graphite/ epoxy composites; 2) chiral composites; 3) omega particulate composites; 4) quasioptic composites; and 5) dielectric composites. Due to the availability of open literature references, the primary focus is constrained of the first two classes: graphite/epoxy and chiral composites. Topics discussed include AC circuit simulation programs; Phase-correction modeling; Wave propagation theory.

ACKNOWLEDGMENTS

The author wishes to extend her sincerest thanks to the following people:

Dave Ross
Don Pflug
Chris Reuter
Tim Blocher
Mike Seifert
Tony Pesta
John Cleary
Dan Kenneally
Ken Siarkiewicz
Ann Buckley
Bill Ward
Linda Wheeler
Luke Miller
Sandy Jablonka

INTRODUCTION

Natural electromagnetic (EM) radiation produced from surrounding environments and radio frequencies emitted from man-made avionics sources interrupt the command and communication signals necessary for desired combatant devices. Knowledge due to meticulous, persistent research has produced state of the art construction of aircraft component systems with advanced composite materials. The achievement of structural and economical goals, such as weight and cost, and electromagnetic compatibility are sought through such theoretical basis as cascading matrices and magnetoelectric coupling. Hence, a theoretical investigation of advanced composite behavior in response to various radio frequencies will certainly lead to superior performance.

The various types of composite materials under investigation are: 1) graphite/epoxy composites; 2) artificially manufactured chiral composites; 3) quasioptic composites; 4) omega particulate composites; and 5) dielectric composites. Graphite/epoxy composites and chiral composites will dominate the focus of this review due to the limited open literature discussion of the other three materials classes.

In order to accurately approximate the controlling properties that effect the electromagnetic response of composite materials, tests must be performed to determine the values of the electromagnetic parameters. Although the various tests are not discussed, the controlling electromagnetic parameters of interest for graphite/epoxy composites are the dielectric permittivity, magnetic permeability and resistance (or conductivity). Once the essential electromagnetic parameters values are known, effective computational analysis is possible.

The controlling electromagnetic parameters for chiral composites are the effective permittivity, effective permeability and the effective chirality parameter. The study of chiral composites in relation to electromagnetic waves has been relatively new due to naturally occurring chirality observed during optical activity. Chiral, "left" or "right" handedness, refers to the natural response of a microscopic particle to rotate polarized light. Since light waves are electromagnetic waves, precise structural and electromagnetic analysis can be used to predict of the phase change induced by chiral composites.

This paper contains four major sections. Section I contains the "Foundational Theory" which structures theoretical arguments such as cascading matrices via Maxwell's equations. Section II describes two theoretical models used to analyze graphite/epoxy composites: 1) the Equivalent-Transmission-Circuit-Line Model and 2) the Filament-Current Phase-Correction Model. Section III provides a brief overview of theories that define the research of helical and omega shaped particles embedded within a dielectric matrix.

I. Foundational Theory: The Reflection and Transmission of EM Waves

Throughout the investigation of improving advanced composite materials, one underlining theory remains the same - the multiplication of cascading matrices. Matrices are the three-dimensional, mathematical representation of the composite structure. A "transmission" matrix multiplied by a vector matrix, composed of incident and reflection coefficients, yield a third matrix that produce an increase or decrease in reflection and incident vector coefficients on a fourth or following matrix. Thus, composites are best modeled as the multiplication of infinite plane matrices in the x and y direction with specified boundary conditions in the z direction. In the following examples, the mathematical processes are outlined for a single-layer, infinite composite slab illuminated by a sinusoidal electromagnetic wave for normal and oblique incidence.

Special Case: Normal Incidence/Homogeneous Isotropic [12], [26]

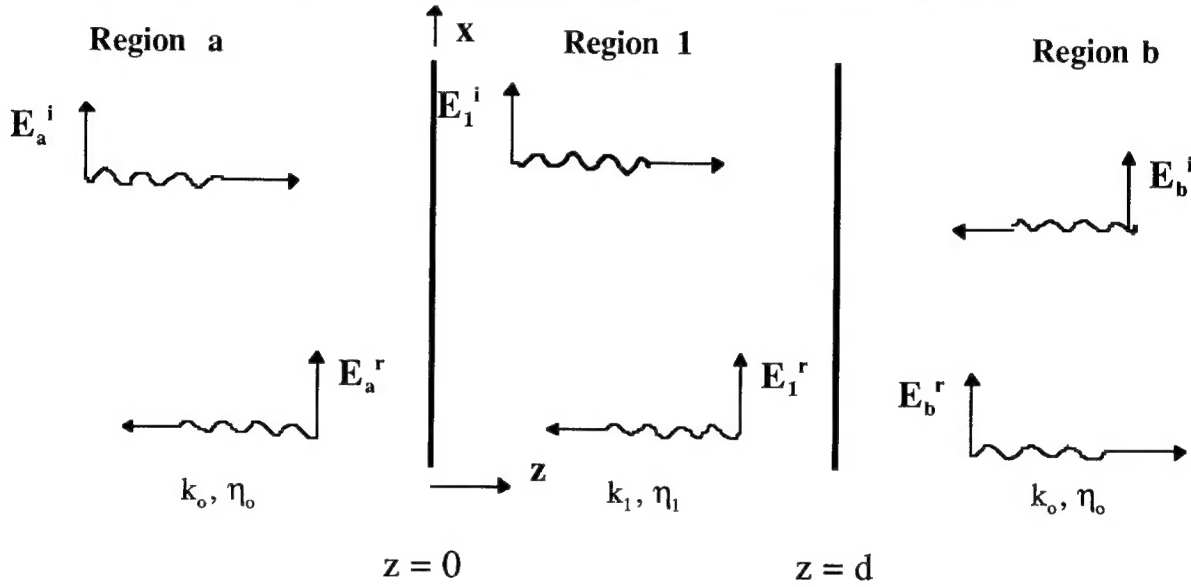


Figure 1-1

Plane wave equations representing the E-fields:

$$\text{Region a: } E_a^i = A_a^i e^{-jk_o z} \mathbf{x} \quad \text{and} \quad E_a^r = A_a^r e^{jk_o z} \mathbf{x}$$

$$\text{Region b: } E_b^r = A_b^r e^{-jk_o(z-d)} \mathbf{x} \quad \text{and} \quad E_b^i = A_b^i e^{jk_o(z-d)} \mathbf{x}$$

$$\text{Composite: } E_1^i = A_1^i e^{-jk_1 z} \mathbf{x} \quad \text{and} \quad E_1^r = A_1^r e^{jk_1 z} \mathbf{x} \quad (\text{Region 1})$$

Plane wave equations representing the H-fields:

$$\text{Region a: } H_a^i = \frac{1}{\eta_o} A_a^i e^{-jk_o z} \mathbf{y} \quad \text{and} \quad H_a^r = -\frac{1}{\eta_o} A_a^r e^{jk_o z} \mathbf{y}$$

$$\text{Region b: } H_b^r = \frac{1}{\eta_o} A_b^r e^{-jk_o(z-d)} \mathbf{y} \quad \text{and} \quad H_b^i = -\frac{1}{\eta_o} A_b^i e^{jk_o(z-d)} \mathbf{y}$$

$$\text{Composite: } H_1^i = \frac{1}{\eta_1} A_1^i e^{-jk_1 z} \mathbf{y} \quad \text{and} \quad H_1^r = -\frac{1}{\eta_1} A_1^r e^{jk_1 z} \mathbf{y} \quad (\text{Region 1})$$

An individual homogeneous conducting layer can be characterized in terms of the tangential electric and magnetic fields in Region a and Region b. These conditions yield the matrix equation:

$$\begin{bmatrix} A_b^r \\ A_b^i \end{bmatrix} = \begin{bmatrix} T_1^{11} & T_1^{12} \\ T_1^{21} & T_1^{22} \end{bmatrix} \begin{bmatrix} A_a^i \\ A_a^r \end{bmatrix}$$

$$T_1^{11} = \frac{(1 + \eta_1)^2}{4\eta_1} [e^{-jk_1 d} - \frac{(1 - \eta_1)^2}{(1 + \eta_1)^2} e^{jk_1 d}]$$

$$T_1^{12} = \frac{(1 - \eta_1)^2}{4\eta_1} (e^{-jk_1 d} - e^{jk_1 d})$$

$$T_1^{21} = -T_1^{12}$$

$$T_1^{22} = \frac{(1 + \eta_1)^2}{4\eta_1} [e^{jk_1 d} - \frac{(1 - \eta_1)^2}{(1 + \eta_1)^2} e^{-jk_1 d}]$$

with $\eta_1 = \eta_1 / \eta_0$.

Thus, the cascading of n isotropic composite layers between the $z = 0$ and $z = d$ interfaces are given by:

$$\begin{bmatrix} A_b^r \\ A_b^i \end{bmatrix} = \left(\prod_{i=1}^n \begin{bmatrix} T_i^{11} & T_i^{12} \\ T_i^{21} & T_i^{22} \end{bmatrix} \right) \begin{bmatrix} A_a^i \\ A_a^r \end{bmatrix}$$

and the ith layer transmission parameters T_i are given by

$$T_i^{11} = \frac{(1 + \eta_i)^2}{4\eta_i} [e^{-jk_i d_i} - \frac{(1 - \eta_i)^2}{(1 + \eta_i)^2} e^{jk_i d_i}]$$

$$T_i^{12} = \frac{(1 - \eta_i)^2}{4\eta_i} (e^{-jk_i d_i} - e^{jk_i d_i})$$

$$T_i^{21} = -T_i^{12}$$

$$T_i^{22} = \frac{(1 + \eta_i)^2}{4\eta_i} [e^{jk_i d_i} - \frac{(1 - \eta_i)^2}{(1 + \eta_i)^2} e^{-jk_i d_i}]$$

with $\eta_i = \eta_i / \eta_0$.

Special Case: Oblique Incidence/Homogeneous Isotropic [12], [26]

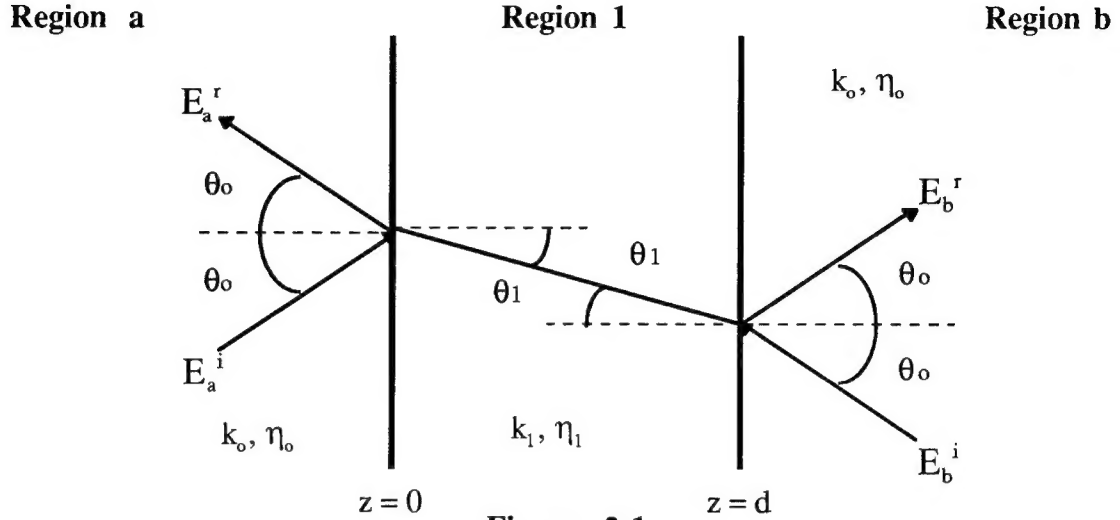


Figure 2-1

For the oblique incidence case, two separate subcases are examined, the transverse electric (TE) case and the transverse magnetic (TM) case. The equations that represent the electric and magnetic field for each case are shown below, following are the respective transmission parameters.

Transverse Electric (TE) Case

The respective electric and magnetic fields for **Region a**:

$$E_a^i = A_a^i e^{-jk_o(z \cos\theta_o + x \sin\theta_o)} [x \cos\theta_o - z \sin\theta_o]$$

$$E_a^r = -A_a^r e^{-jk_o(-z \cos\theta_o + x \sin\theta_o)} [x \cos\theta_o + z \sin\theta_o]$$

$$H_a^i = \frac{1}{\eta_o} A_a^i e^{-jk_o(x \sin\theta_o + z \cos\theta_o)} y$$

$$H_a^r = \frac{1}{\eta_o} A_a^r e^{-jk_o(-z \cos\theta_o + x \sin\theta_o)} y$$

The respective electric and magnetic fields for **Region b**:

$$E_b^i = -A_b^i e^{-jk_o(x \sin\theta_o + (z-d) \cos\theta_o)} [x \cos\theta_o + z \sin\theta_o]$$

$$E_b^r = A_b^r e^{-jk_o(x \sin\theta_o + (z-d) \sin\theta_o)} [x \cos\theta_o - z \sin\theta_o]$$

$$H_b^i = \frac{1}{\eta_o} A_b^i e^{-jk_o(x \sin\theta_o - (z-d) \cos\theta_o)} y$$

$$H_b^r = \frac{1}{\eta_o} A_b^r e^{-jk_o(x \sin\theta_o + (z-d) \cos\theta_o)} y$$

The respective equations that relate Region a with Region 1 at the $z = 0$ interface are:

$$B_1 = 1/2 (\eta_1 + 1/v_1) A_a^i + 1/2 (\eta_1 - 1/v_1) A_a^r$$

$$C_1 = 1/2 (\eta_1 - 1/v_1) A_a^i + 1/2 (\eta_1 + 1/v_1) A_a^r$$

The respective equations that relate Region 1 with Region b at the $z = d$ interface are:

$$B_1 = 1/2 (\eta_1 - 1/v_1) A_b^i e^{jk_1 d \cos \theta_1} + 1/2 (\eta_1 + 1/v_1) A_b^r e^{jk_1 d \cos \theta_1}$$

$$C_1 = 1/2 (\eta_1 + 1/v_1) A_b^i e^{-jk_1 d \cos \theta_1} + 1/2 (\eta_1 - 1/v_1) A_b^r e^{-jk_1 d \cos \theta_1}$$

Therefore, transmission parameters, T_i , for the transverse electric (TE) case of a composite slab of i th layers are given by:

$$T_i^{11} = \frac{(1 + \eta_i v_i)^2}{4\eta_i v_i} (e^{-jk_i d_i \cos \theta_i} - \frac{(1 - \eta_i v_i)^2}{(1 + \eta_i v_i)^2} e^{jk_i d_i \cos \theta_i})$$

$$T_i^{12} = \frac{1 - (\eta_i v_i)^2}{4\eta_i v_i} (e^{-jk_i d_i \cos \theta_i} - e^{jk_i d_i \cos \theta_i})$$

$$T_i^{21} = -T_i^{12}$$

$$T_i^{22} = \frac{(1 + \eta_i v_i)^2}{4\eta_i v_i} (e^{jk_i d_i \cos \theta_i} - \frac{(1 - \eta_i v_i)^2}{(1 + \eta_i v_i)^2} e^{-jk_i d_i \cos \theta_i})$$

where $\theta_i = \sin^{-1} (k_o/k_i \sin \theta_o)$

$$\eta_i = \eta_i / \eta_o$$

$$v_i = \cos \theta_i / \cos \theta_o$$

Transverse Magnetic (TM) Case

The respective electric and magnetic fields for **Region a**:

$$E_a^i = A_a^i e^{-jk_o(z \cos \theta_o + x \sin \theta_o)} \mathbf{y}$$

$$E_a^r = A_a^r e^{-jk_o(-z \cos \theta_o + x \sin \theta_o)} \mathbf{y}$$

$$H_a^i = \frac{1}{\eta_o} A_a^i e^{-jk_o(z \cos \theta_o + x \sin \theta_o)} [-x \cos \theta_o + z \sin \theta_o]$$

$$H_a^r = \frac{1}{\eta_o} A_a^r e^{-jk_o(-z \cos \theta_o + x \sin \theta_o)} [x \cos \theta_o + z \sin \theta_o]$$

The respective electric and magnetic fields for **Region b**:

$$E_b^i = -A_b^i e^{-jk_o(-(z-d) \cos\theta_o + x \sin\theta_o)} \mathbf{y}$$

$$E_b^r = A_b^r e^{-jk_o((z-d) \sin\theta_o + x \sin\theta_o)} \mathbf{y}$$

$$H_b^i = \frac{1}{\eta_o} A_b^i e^{-jk_o((z-d)\cos\theta_o + x \sin\theta_o)} [x \cos\theta_o + z \sin\theta_o]$$

$$H_b^r = \frac{1}{\eta_o} A_b^r e^{-jk_o((z-d) \cos\theta_o + x \sin\theta_o)} [-x \cos\theta_o + z \sin\theta_o]$$

The respective equations that relate Region a with Region 1 at the $z = 0$ interface:

$$B_1 = 1/2 (1 + \eta_1 / \nu_1) A_a^i + 1/2 (1 - \eta_1 / \nu_1) A_a^r$$

$$C_1 = 1/2 (1 - \eta_1 / \nu_1) A_a^i + 1/2 (1 + \eta_1 / \nu_1) A_a^r$$

The respective equations that relate Region 1 with Region b at the $z = d$ interface:

$$B_1 = 1/2 (1 - \eta_1 / \nu_1) A_b^i e^{jk_1 d \cos\theta_1} + 1/2 (1 + \eta_1 / \nu_1) A_b^r e^{jk_1 d \cos\theta_1}$$

$$C_1 = 1/2 (\eta_1 / \nu_1 + 1) A_b^i e^{-jk_1 d \cos\theta_1} + 1/2 (-\eta_1 / \nu_1 + 1) A_b^r e^{-jk_1 d \cos\theta_1}$$

Therefore, transmission parameters, T_i , for the transverse magnetic (TM) case of a composite slab of i th layers are given by

$$T_i^{11} = \frac{(\eta_i + \nu_i)^2}{4\eta_i \nu_i} (e^{-jk_i d_i \cos\theta_i} - \frac{(\eta_i - \nu_i)^2}{(\eta_i + \nu_i)^2} e^{jk_i d_i \cos\theta_i})$$

$$T_i^{12} = \frac{(\eta_i - \nu_i)^2}{4\eta_i \nu_i} (e^{jk_i d_i \cos\theta_i} - e^{-jk_i d_i \cos\theta_i})$$

$$T_i^{21} = -T_i^{12}$$

$$T_i^{22} = \frac{(\eta_i + \nu_i)^2}{4\eta_i \nu_i} (e^{jk_i d_i \cos\theta_i} - \frac{(\eta_i - \nu_i)^2}{(\eta_i + \nu_i)^2} e^{-jk_i d_i \cos\theta_i})$$

where $\theta_i = \sin^{-1} (k_o / k_i \sin \theta_o)$

$$\eta_i = \eta_i / \eta_o$$

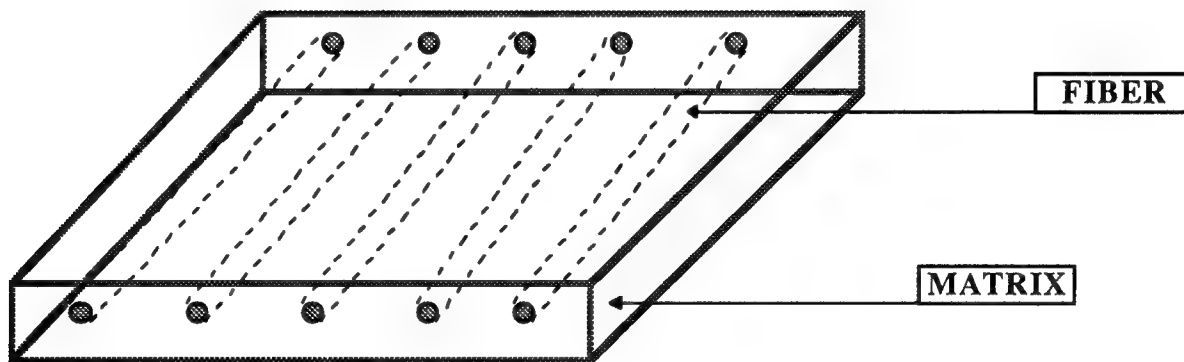
$$1/\nu_i = \cos\theta_o / \cos\theta_i.$$

Corresponding formulas for the anisotropic/ normal incidence and anisotropic oblique incidence are given in reference [26].

II. Graphite/Epoxy Composites

The first composite class discussed in this paper are anisotropic carbon fiber composites (CFC). The carbon fiber composites (Figure 1-2) normally utilized in most aerospace applications are the graphite/ epoxy (G/E) composites. The special properties in specific directions are designed by choosing the required fiber and matrix. However, the most important mechanical properties are the specific tensile strength or specific modulus. These properties are the central to design decisions for aircraft applications because they present the ratio of strength (or stiffness) to weight [12].

Figure 1-2 Schematic Diagram of CFC [12]



In addition to the composite fiber, the composite matrix properties, in the form of resin, performs two important tasks: (1) separation of fibers to maximize their contributions to strength and minimize the possibility of cracks and buckling caused from fibers in contact and (2) enabling the transfer of stresses between fibers by sufficiently binding the fibers throughout the material.

The following two sections outline the basic formulation of the Equivalent-Transmission-Circuit-Line (ETCL) model and the Filament-Current Phase Correction (FCPC) model for graphite/epoxy composites.

II. A. The Equivalent-Transmission-Circuit-Line Model

An equivalent-transmission-circuit-line model represents the electric- and magnetic-field responses of graphite/ epoxy composites to radio frequencies as a complex yet simple circuit of alternating current. In addition to the electromagnetic properties of permittivity (ϵ), permeability (μ) and conductivity (σ); inductance (L), capacitance (C) and conductance (G) properties are utilized to describe transient propagation of plane waves through composite structures. Hence, graphite/ epoxy composites are characterized as a combination of semiconducting and/or insulating material.

The wave-transmission-matrix (WTM) method was initially used to construct the solution of frequency-domain Maxwell's equations for laminated anisotropic composites illuminated by an obliquely incident plane wave. By imposing the necessary boundary conditions on the interfaces, and finally cascading the wave-transmission matrix for each lamina, a derivation was developed for the relationships between the incident, reflected, and transmitted field [24]. In the following problem statements, a brief analysis of anisotropic homogeneous and anisotropic inhomogeneous laminates are given for graphite/epoxy composites.

II. A. 1. Frequency-Domain Analysis of Graphite/Epoxy Composites

II. A. 1. a. Special Case: Anisotropic Homogeneous Laminates [24]

Problem Statement

Consider a composite structure with M number of layers, each described by discrete electromagnetic properties such as permeability μ_0 , anisotropic permittivity ϵ_m , and conductivity σ_m . (Figure 1, Appendix A). Where the permeability is essentially uniform, while the permittivity and conductivity are expressed as tensors in the following form:

$$\epsilon_m = \begin{bmatrix} \epsilon_{xx} & \epsilon_{xy} & 0 \\ \epsilon_{yx} & \epsilon_{yy} & 0 \\ 0 & 0 & \epsilon_{zz} \end{bmatrix}_m \quad \sigma_m = \begin{bmatrix} \sigma_{xx} & \sigma_{xy} & 0 \\ \sigma_{yx} & \sigma_{yy} & 0 \\ 0 & 0 & \sigma_{zz} \end{bmatrix}_m$$

Here

$$\begin{aligned} \epsilon_{xx} &= \epsilon_x \cos^2 \phi + \epsilon_y \sin^2 \phi \\ \epsilon_{xy} &= \epsilon_{yx} = (\epsilon_x - \epsilon_y) \cos \phi \sin \phi \\ \epsilon_{yy} &= \epsilon_x \sin^2 \phi + \epsilon_y \cos^2 \phi \\ \epsilon_{zz} &= \epsilon_z \end{aligned}$$

The primed parameters of permittivity are the composite principal axes and ϕ is the angle between the global and the principal axis (Figure 2-2). The expressions for the conductivities are similar to those used for the respective permittivities (σ_{xx} , $\sigma_{xy} = \sigma_{yx}$, σ_{yy} , σ_{zz}).

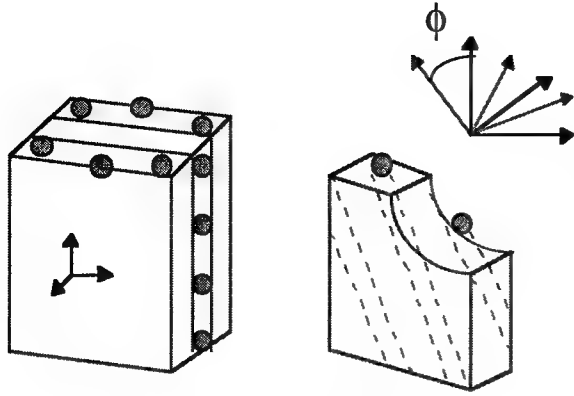


Figure 2-2
Global coordinates (black coordinate axis) and principal coordinates (gray coordinate axis) for laminated composites [24].

The circuit simulation program, PSPICE, has been used to perform the numerical analysis of the ETCL model. However, before subjecting the ETCL model to a simulation program, the transmission lines must be individualized and their values estimated by cascading π - and T-circuit sections as either π -T- π or T- π -T circuit models (Figure 2, Appendix A). According to reference [24], the π -T- π circuit model produces better convergence and numerical stability than the T- π -T circuit model.

In the analysis of the ETCL model a composite lamina of length d contains an odd number, $2m + 1$, of π - and T- circuit sections, where m is the number of laminae of length d within the single-composite layer. Assuming the same method applied to inhomogeneous composites, an accurate convergence of the π -T- π circuit model may be obtained by calculating N number of circuit sections (where $N = 2m + 1$). The total length of the π -T- π circuit section is characterized by a length l where the π -section (l_1) is half the length of T-section (l_2) of the circuit [15]. For the ETCL model, the length of the π - and T-sections should be less than half the effective skin depth, where the skin depth is a function of effective conductivity and frequency [24].

$$\delta_{\text{eff}} = \sqrt{\frac{1}{\pi f \mu_0 \sigma_{\text{eff}}}}$$

The appropriate coupled transmission line equations for the homogeneous anisotropic ETCL model are:

$$\frac{\partial v}{\partial z} = -L \cdot \frac{\partial \epsilon}{\partial t}$$

$$\frac{\partial \epsilon}{\partial z} = -(C \frac{\partial v}{\partial t} + G) \cdot v$$

The equivalent inductance, capacitance, and conductance matrices in the coupled transmission line equations for the homogeneous case are:

$$L = \mu_0 \begin{bmatrix} 1 - \sin^2 \theta & 0 \\ \epsilon_{zz} & 1 \end{bmatrix}$$

$$C = \epsilon_0 \begin{bmatrix} \epsilon_{xx} & -\epsilon_{xy} \\ -\epsilon_{xy} & \epsilon_{yy} - \sin^2 \theta \end{bmatrix}$$

$$\mathbf{G} = \begin{bmatrix} \sigma_{xx} & -\sigma_{xy} \\ -\sigma_{xy} & \sigma_{yy} \end{bmatrix}$$

the necessary boundary conditions for the voltage and current are given by:

$$v_p(0, t) + \eta_p \epsilon_p(0, t) = 2v_p'(t) \quad \text{at incident boundary}$$

where $p = ||$ or \perp

$$v_p(D, t) + \eta_p \epsilon_p(D, t) = 0 \quad \text{at transmitted boundary}$$

Where ' p ' denotes the parallel component or the perpendicular E-field of the plane wave to the x-z plane of incidence. The voltage and current wave vectors are defined as in [24]:

$$\mathbf{v}(z, t) = \begin{bmatrix} v_{||} \\ v_{\perp} \end{bmatrix} = \begin{bmatrix} \mathcal{E}_x \\ -\mathcal{E}_y \end{bmatrix}_{x=0} = \int_{-\infty}^{\infty} \begin{bmatrix} E_x(z; \omega) \\ -E_y(z; \omega) \end{bmatrix} e^{j\omega t} d\omega$$

$$\mathbf{i}(z, t) = \begin{bmatrix} i_{||} \\ i_{\perp} \end{bmatrix} = \begin{bmatrix} \mathcal{H}_x \\ -\mathcal{H}_y \end{bmatrix}_{x=0} = \int_{-\infty}^{\infty} \begin{bmatrix} H_x(z; \omega) \\ -H_y(z; \omega) \end{bmatrix} e^{j\omega t} d\omega$$

Here the transient waveform as a function of the incident angle θ for the plane wave can be expressed as:

$$\mathcal{E}(x, z, t) = \int_{-\infty}^{\infty} E(z; \omega) e^{j\omega t} e^{-jk_0 x \sin\theta} d\omega$$

$$\mathcal{H}(x, z, t) = \int_{-\infty}^{\infty} H(z; \omega) e^{j\omega t} e^{-jk_0 x \sin\theta} d\omega$$

where $k_0 = \omega \sqrt{\mu_0 \epsilon_0} = \omega / c$ is the free-space wavenumber and c is the velocity of light.

The combination of the ETCL model and the wave-transmission-matrix (WTM) method can be used to predict the transmittivity and reflectivity terms which are basically mathematical expressions of the transient plane wave behavior within a composite structure. In the PSPICE simulation program, the command ".AC", conducts the frequency-domain analysis. The transmittivity coefficients $T_{||,||}$, $T_{||,\perp}$, $T_{\perp,\perp}$, and $T_{\perp,||}$ and the reflectivity coefficients $R_{||,||}$, $R_{||,\perp}$, $R_{\perp,\perp}$, and $R_{\perp,||}$ in the frequency-domain are given by the following definitions [24]:

$$T_{p,q} = \frac{E^t_{p,q}}{E^i_p} \quad R_{p,q} = \frac{E^r_{p,q}}{E^i_p}$$

An estimation of the copolarization term for transmittivity in the lower frequency range for specific case where each lamina has equal thickness is given by:

$$T_{p,p} = \frac{2}{\eta_p \sigma_{\text{eff}} M d}$$

where η_p , the characteristic impedance of the incident wave, is given by $\eta_{||} = \eta_0 \cos\theta$ and $\eta_{\perp} = \eta_0 / \cos\theta$ for the $E_{||}$ and E_{\perp} wave, respectively; and $\eta_0 = \sqrt{\mu_0 / \epsilon_0}$ is the intrinsic impedance of the free space [24].

$$\sigma_{\text{eff}} = \frac{1}{M} \left[\sum_{m=1}^M (\sigma_{\text{eff}})_m \right]$$

$(\sigma_{\text{eff}})_m$ (ohm/m) is the effective conductivity of the mth ply within the composite structure. This can be described by the corresponding formulas for the $E_{||}$ and E_{\perp} wave respectively as:

$$(\sigma_{\text{eff}})_m = \begin{cases} (\sigma_x)_m \cos^2 \phi + (\sigma_y)_m \sin^2 \phi, & \text{for } E_{||} \text{ wave} \\ (\sigma_x)_m \sin^2 \phi + (\sigma_y)_m \cos^2 \phi, & \text{for } E_{\perp} \text{ wave.} \end{cases}$$

Note: Although the formula for the cross-polarization terms are not given, when a wave performs multiple reflections in a region, the cross-polarization terms will be dominant if the thickness of the region is near a quarter-wavelength [24].

II. A. 1. b. Special Case: Anisotropic Inhomogeneous Laminates [15]

Problem Statement

Consider a composite structure with one-layer of length, D . The electromagnetic properties of the slab, such as permittivity, permeability and conductivity are described as tensors and expressed in the following form:

$$\boldsymbol{\epsilon} = \begin{bmatrix} \epsilon_{xx} & \epsilon_{xy} & 0 \\ \epsilon_{yx} & \epsilon_{yy} & 0 \\ 0 & 0 & \epsilon_{zz} \end{bmatrix} \quad \boldsymbol{\mu} = \begin{bmatrix} \mu_{xx} & \mu_{xy} & 0 \\ \mu_{yx} & \mu_{yy} & 0 \\ 0 & 0 & \mu_{zz} \end{bmatrix}$$

$$\boldsymbol{\sigma} = \begin{bmatrix} \sigma_{xx} & \sigma_{xy} & 0 \\ \sigma_{yx} & \sigma_{yy} & 0 \\ 0 & 0 & \sigma_{zz} \end{bmatrix}.$$

These tensors are assumed to be a function of z , but independent of frequency. The governing equations for the transverse field components are given by:

$$\frac{\partial}{\partial z} \mathbf{v} = -\mathbf{L} \cdot \frac{\partial}{\partial t} \boldsymbol{\epsilon}$$

$$\frac{\partial}{\partial z} \boldsymbol{\epsilon} = -(\mathbf{C} \frac{\partial}{\partial t} + \mathbf{G}) \cdot \mathbf{v}$$

Where

$$\mathbf{L} = \mu_0 \begin{bmatrix} 1 - \sin^2 \theta & 0 \\ \epsilon_{zz} & 1 \end{bmatrix} \quad \mathbf{C} = \epsilon_0 \begin{bmatrix} \epsilon_{xx} & -\epsilon_{xy} \\ -\epsilon_{xy} & \epsilon_{yy} - \sin^2 \theta \end{bmatrix}$$

$$\mathbf{G} = \begin{bmatrix} \sigma_{xx} & -\sigma_{xy} \\ -\sigma_{xy} & \sigma_{yy} \end{bmatrix}$$

The incident plane is chosen to be the x-z plane with an incident angle of θ and arbitrary transient waveform. The plane wave is divided into two components which are the parallel and perpendicular electric-field in reference to the plane of incidence, represented by $E_{||}$ and E_{\perp} respectively. Considering the fields at the $x=0$ plane, the voltage and current wave vectors are defined as:

$$\mathbf{v}(z, t) = \begin{bmatrix} v_{||} \\ v_{\perp} \end{bmatrix} = \begin{bmatrix} \mathcal{E}_x \\ -\mathcal{E}_y \end{bmatrix}_{x=0}$$

$$\mathbf{i}(z, t) = \begin{bmatrix} i_{||} \\ i_{\perp} \end{bmatrix} = \begin{bmatrix} \mathcal{H}_x \\ -\mathcal{H}_y \end{bmatrix}_{x=0}$$

Last and most important, the necessary boundary conditions can be stated as follows

$$v_p(0, t) + \eta_p i_p(0, t) = 2v_p'(t) \quad \text{at incident boundary} \quad \text{where } p = || \text{ or } \perp$$

$$v_p(D, t) + \eta_p i_p(D, t) = 0 \quad \text{at transmitted boundary.}$$

II. A. 2. Time-Domain Analysis of Graphite/ Epoxy Composites

Special Case: Incident Transient Pulse, EMP

A specific type of electromagnetic radiation produced from surrounding natural or man-made environments is the electromagnetic pulse (EMP). For this case, consider the field $\mathcal{E}(z, t)$ at $x=0$ plane, under an obliquely incident, electromagnetic pulse waveform $\mathcal{E}'(t)$ given by

$$\mathcal{E}'(t) = E_o (e^{-\alpha t} - e^{-\beta t}) u(t)$$

here $u(t) = 1$ for $t > 0$. Also, the values of $E_o = 1/(e^{-\alpha t_o} - e^{-\beta t_o})$ and $t_o = \ln(\beta/\alpha)/(\beta-\alpha)$ [24]. When plotting incident electromagnetic pulse versus time or frequency, the values of α and β determine the shape and frequency spectrum of the EM pulse.

II. B. The Filament-Current Phase-Correction Model [14]

The goal of the filament-current phase correction model is to reduce the unpredictable scattering patterns which disrupt communication and control signals utilized by various applications. The electric-field radiated by a fiber embedded within the dielectric matrix and the electric-field resulting from the incident plane wave, constitute the total electric-field produced by the composite structure. The electric-field resulting from the incident plane wave can be expressed as:

$$E^{inc} = \exp(-i k x \sin \theta + i k y \cos \theta)$$

while the scattered electric-field resulting from the fiber embedded within the dielectric matrix can be expressed by the equation

$$E^s \equiv -\frac{k \eta I_f}{4} D(x, y)$$

where $\eta = \sqrt{\mu_o / (\epsilon_o \epsilon_r)}$ and

$$D(x, y) = \sum_{n=-\infty}^{\infty} \frac{2 i \exp(-\alpha_n |y|)}{\alpha_n d} \exp(-i k_n x)$$

here

$$k_n = k \sin \theta + \frac{2n\pi}{d}$$

$$\alpha_n = \begin{cases} i \sqrt{k^2 - k_n^2} & \text{if } k^2 > k_n^2 \\ \sqrt{k_n^2 - k^2} & \text{if } k^2 < k_n^2 \end{cases}$$

In this analysis the composite structure is described by a periodic fiber-matrix (Figure 3-2). The total electric-field can be substituted into an equation representative of the concentrated electric current along the center of the conducting fiber.

$$I_f = \iint_A J \, dx \, dy = \iint_A \sigma E \, dx \, dy$$

where E is the total field and A is the fiber area.

From this approximation of the electric current, the reflected and transmitted electric-field can be computed.

$$I_f = \frac{\sigma \iint_A \exp(-ikx \sin \theta + ik y \cos \theta) dx dy}{1 + \frac{\sigma k \eta}{4} \iint_A \sum_{n=-\infty}^{\infty} \frac{2i \exp(-\alpha_n |y|)}{\alpha_n d} \exp(-ik_n x) dx dy}$$

The relation between the reflected and transmitted electric-field, approximated electric current and phase-correction model follow in the succeeding discussion.

The phase-correction model follows the logic of the foundational theory, the multiplication of matrices. In reference to the equation for the scattered electric-field, the Fourier transform, $D(x, y)$, contains an infinite number of discrete terms numbered as individual Floquet modes. The computations for the phase-correction model are formulated for a single Floquet-layer within a composite structure (Figure 4-2), where the Floquet layer contains $2m + 1$ Floquet modes.

The incident wave that illuminates the composite on the initial free space/ dielectric interface is represented by the vector A_1

$$A_1 = [E_{-m} \ E_{-m+1} \ \dots \ E_0 \ \dots \ E_{m-1} \ E_m]^T$$

Where E_l ($l = -m, \dots, 0, \dots, m$) is the amplitude of the l th Floquet mode and the superscript T denotes the transpose [14]. The same principle follows for the vectors A_2, \dots, A_6 and B_1, \dots, B_6 within the $2m + 1$ Floquet modes.

Thus, the reflection and transmission phenomena at the air-matrix interfaces may be represented by

$$\begin{bmatrix} B_1 \\ B_2 \end{bmatrix} = \begin{bmatrix} R_{fd} & T_{df} \\ T_{fd} & R_{df} \end{bmatrix} \begin{bmatrix} A_1 \\ A_2 \end{bmatrix},$$

$$\begin{bmatrix} B_5 \\ B_6 \end{bmatrix} = \begin{bmatrix} R_{df} & T_{fd} \\ T_{df} & R_{fd} \end{bmatrix} \begin{bmatrix} A_5 \\ A_6 \end{bmatrix}$$

and those at the Floquet layer (fiber grating) by

$$\begin{bmatrix} B_3 \\ B_4 \end{bmatrix} = \begin{bmatrix} R & T \\ T & R \end{bmatrix} \begin{bmatrix} A_3 \\ A_4 \end{bmatrix}$$

The subscripts fd for the R and T coefficients are the respective diagonal reflection and transmission matrices from free space to the dielectric matrix, and the subscripts df for the R and T coefficients are the respective diagonal reflection and transmission matrices from the dielectric matrix to free space.

The relationship between the wave vectors A_i and B_i (where $i = 1, 2, \dots, 5, 6$) and the phase shift may be expressed by the multiplication of the following matrices:

$$\begin{bmatrix} B_3 \\ A_3 \end{bmatrix} = \begin{bmatrix} P+ & 0 \\ 0 & P- \end{bmatrix} \begin{bmatrix} A_2 \\ B_2 \end{bmatrix}$$

$$\begin{bmatrix} A_5 \\ B_5 \end{bmatrix} = \begin{bmatrix} P- & 0 \\ 0 & P+ \end{bmatrix} \begin{bmatrix} A_4 \\ B_4 \end{bmatrix}$$

Where

$P+ =$ a diagonal matrix with dimensions $(2m+1) \times (2m+1)$, whose i th element is $\exp [t_{\alpha-(m+1)}/2]$

$P- =$ the complex conjugate of $P+$

Let a combination of the above matrices be represented by the four full matrices M_{11} , M_{16} , M_{61} , and M_{66} (analogous to the transmission coefficients T_i^{11} , T_i^{12} , T_i^{21} , and T_i^{22}). The combination of the above matrices are represented by cascading the vectors $[B_1 \ B_6]^T$ and $[A_1 \ A_6]^T$ expressed by the following relationship

$$\begin{bmatrix} B_1 \\ B_6 \end{bmatrix} = \begin{bmatrix} M_{11} & M_{16} \\ M_{61} & M_{66} \end{bmatrix} \begin{bmatrix} A_1 \\ A_6 \end{bmatrix} \quad [14].$$

Thus, the ETCL model and the FCPC model parallel in three different areas: 1) Theoretical Basis; 2) Structural Modeling and 3) Fundamental Compartmentalization. The theoretical basis for both models are the same, cascading matrices. The structural modeling for the ETCL model is an AC circuit, while a periodic fiber-matrix describes the FCPC model. Finally, the fundamental compartmentalization for the ETCL model and the FCPC model is $2m+1$ T- and π - circuit sections and the $2m+1$ Floquet modes, respectively. This information has been tabulated in Table 4.

Table 4 Summary of ETCL and FCPC model

	ETCL Model	FCPC Model
Theoretical Basis	Cascading Matrices	Cascading Matrices
Structural Modeling	AC Circuit	Periodic Fiber-Matrix
Fundamental Compartmentalization	$2m+1$ T- and π - circuits	$2m+1$ Floquet modes

Phase-Correction Model for Graphite/Epoxy Composite

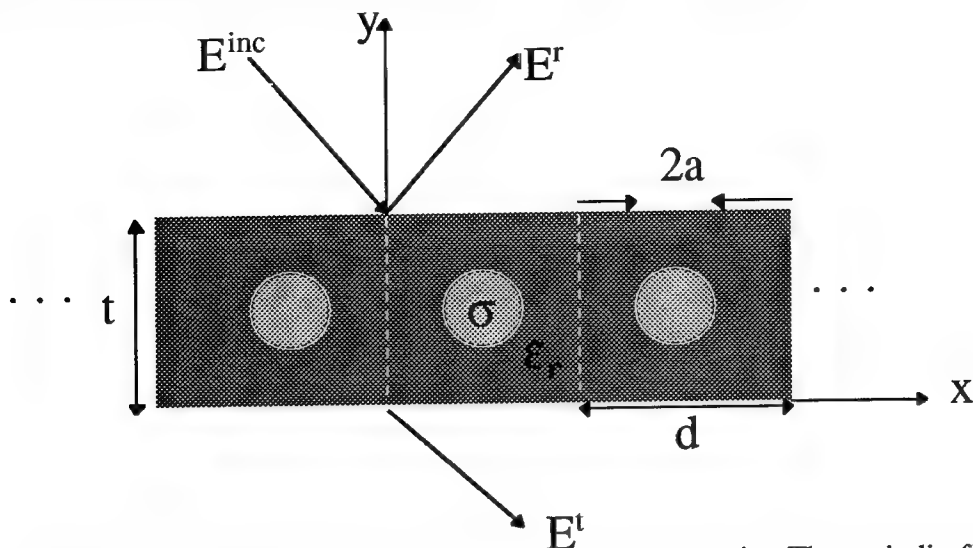


Figure 3-2. Geometry of a lossy, single-layer G/E composite. The periodic-fiber matrix (graphite) of radius a and conductivity σ embedded in dielectric matrix (epoxy) of thickness t and relative permittivity ϵ_r .

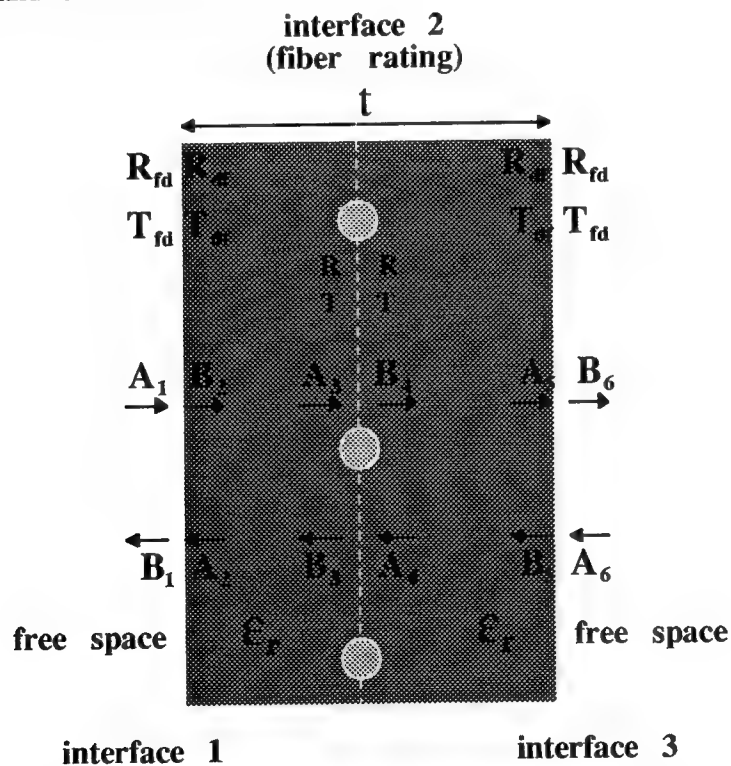


Figure 4-2. Phase-correction model for multi-mode reflection and transmission due to fiber grating within a dielectric matrix.

III. Chiral Composites

III. A. Brief History

In 1812, Biot observed the phenomenon of optical rotation, or more appropriately termed, optical activity. Optical activity occurred when white linearly polarized light changes to a rainbow of colors when shown through the crystal, quartz [21]. In 1848, Pasteur accredited the rotation of plane polarized light and the observation of the two forms of tartaric acid salts to the handedness of the material's microstructure [25]. The term chiral comes from the Greek word $\chi\rho\omicron$, which means "hand" or a typical mirror-asymmetrical object [9]. In the early 1900's, Lindman discovered the handedness, chirality, of artificially constructed materials. His measurements of plane polarization through a collection of wire helices in a lower frequency range have established studies of observed rotation and absorption of electromagnetic waves in dielectric material, since light is an electromagnetic wave [21], [25]. In 1956, Winkler performed similar experiments with 200 randomly oriented right-handed copper helices embedded in a dielectric matrix, but concluded the measurements of plane rotation were due to diffraction effects rather than optical activity [10], [21]. He found that over a frequency band from 1.5 to 2.7 Ghz the electric field of a linearly polarized wave was rotated by angles varying from 0 to 12 degrees.

Later in 1957 and 1960, Tinoco and Freeman conducted numerous measurements of effectively anisotropic chiral material. They discovered that illumination of a composite, consisting of right handed helices oriented parallel to the direction of propagation, yields an electric field with an angle variation from 0 to 30 degrees in the frequency range of 8.3 to 11.5 Ghz. The resonance band frequency of 12.5 Ghz yields rotated angles varying from 30 to 180 degrees [10]. Winkler, Tinoco, and Freeman all assumed the light remained linearly polarized after leaving springs, since they lacked the equipment used to measure copolarized and cross-polarized components of the transmitted elliptically polarized waves [10]. In 1974, Bohren introduced the decomposition of electromagnetic waves into left and right circularly polarized fields [21]. Therefore, the wave leaving a medium of springs, of the same handedness, was usually elliptically polarized [10].

Since then, the discovery of chiral helices has expanded to inclusion shapes such as omega particles [17]. Once a solid theoretical and economical basis has been formed chiral composites might be utilized as a advance in the control of electromagnetic interference. The following section is a brief synopsis of the various theories related to chiral composites.

III. B. 1. Theoretical Approaches

Numerous approaches have been developed to account for the behavior of chiral composites. The first approach discussed in this section, the Waterman-Truell approach [11] analyzes the dielectric-dielectric composite in which chiral particles are made of chiral material but do not necessarily possess chiral shape. This approach assumes a homogenized medium with no interaction between the microscopic particles. The argument begins by stating equations for point dipoles at the origin and then relating the scattered electric and magnetic fields to the average dipole moments.

From previous studies, medium characterized by the above relations is isotropic chiral. As mentioned before, propagation in chiral material produces elliptically left (+) and right (-) circularly polarized plane waves. The circularly polarized plane waves for the respective incident electric and magnetic fields are:

$$\mathbf{E}_{inc}(\mathbf{r}) = (1/\sqrt{2})(\mathbf{u}_x \pm i\mathbf{u}_y) \exp(ik_0 z)$$

$$\mathbf{H}_{inc}(\mathbf{r}) = \pm(1/i\eta\sqrt{2})(\mathbf{u}_x \pm i\mathbf{u}_y) \exp(ik_0 z)$$

therefore the average dipole moments for the circularly polarized plane waves are given by:

$$\mathbf{p} = (1/\sqrt{2})(\alpha_{ee} \pm \alpha_{eh}/\eta_0)(\mathbf{u}_x \pm i\mathbf{u}_y)$$

$$\mathbf{m} = \pm(1/i\eta_0\sqrt{2})(\alpha_{hh} \pm \alpha_{eh}\eta_0)(\mathbf{u}_x \pm i\mathbf{u}_y).$$

By examining the electric field in the far zone, the following limit can be stated as:

$$\lim_{k_0 r \rightarrow \infty} \mathbf{E}(\mathbf{r}) = \omega\{\omega\mu_0[\mathbf{p} - \mathbf{u}_r(\mathbf{p} \cdot \mathbf{u}_r)] - k_0\mathbf{u}_r \times \mathbf{m}\} \{\exp(ik_0 r)/4\pi r\}$$

The forward and backward plane-wave scattering amplitude can then be described by the equations:

$$\mathbf{F}_{forw} = (\omega^2/4\pi)(1/\sqrt{2})(\mathbf{u}_x \pm i\mathbf{u}_y) \{\mu_0(\alpha_{ee} \pm \alpha_{eh}/\eta_0) + \epsilon_0(\alpha_{hh} \pm \alpha_{eh}\eta_0)\}$$

$$\mathbf{F}_{back} = (\omega^2/4\pi)(1/\sqrt{2})(\mathbf{u}_x \pm i\mathbf{u}_y) \{\mu_0(\alpha_{ee} \pm \alpha_{eh}/\eta_0) - \epsilon_0(\alpha_{hh} \pm \alpha_{eh}\eta_0)\}$$

and the wavenumbers for the left (+) and right (-) polarized wave according to the Waterman-Trueell approach are:

$$\gamma_{WT \pm} = k_0 \sqrt{\{1 + (\omega N/k_0^2)[\omega(\mu_0\alpha_{ee} + \epsilon_0\alpha_{hh}) \pm 2k_0\alpha_{eh}] + (\omega N/k_0)^2[\alpha_{ee}\alpha_{hh} + \alpha_{eh}(\alpha_{ee}\eta_0 + \alpha_{hh}/\eta_0)]\}}.$$

The Maxwell Garnett approach [11] derived constitutive relations for the homogenized chiral medium in the form of bulk parameters. The effects of electromagnetic radio waves was examined in the low frequency range. Each chiral particle has been encapsulated in a bianisotropic sphere which is described by the Tellegen chirality parameter. Thus, isotropic chiral medium adhere to the following Tellegen constitutive relations given by the respective electric and magnetic flux densities

$$\mathbf{D} = \epsilon_{MG} \mathbf{E} + \zeta_{MG} \mathbf{H}$$

$$\mathbf{B} = \mu_{MG} \mathbf{H} - \zeta_{MG} \mathbf{E}$$

where

$$\epsilon_{MG} = \epsilon_0 \frac{[9\mu_0\epsilon_0 - 3N(\epsilon_0\alpha_{hh} - 2\mu_0\alpha_{ee}) - 2N^2(\alpha_{ee}\alpha_{hh} - \alpha_{eh}^2)]}{[9\mu_0\epsilon_0 - 3N(\epsilon_0\alpha_{hh} + 2\mu_0\alpha_{ee}) + 2N^2(\alpha_{ee}\alpha_{hh} - \alpha_{eh}^2)]}$$

is the permittivity,

$$\mu_{MG} = \mu_0 \frac{[9\mu_0\epsilon_0 - 3N(\mu_0\alpha_{ee} - 2\epsilon_0\alpha_{hh}) - 2N^2(\alpha_{ee}\alpha_{hh} - \alpha_{eh}^2)]}{[9\mu_0\epsilon_0 - 3N(\epsilon_0\alpha_{hh} + 2\mu_0\alpha_{ee}) + 2N^2(\alpha_{ee}\alpha_{hh} - \alpha_{eh}^2)]}$$

is the permeability,

$$\zeta_{MG} = i \frac{9\mu_o \epsilon_o N\alpha_{eh}}{[9\mu_o \epsilon_o - 3N(\epsilon_o \alpha_{hh} + 2\mu_o \alpha_{ee}) + 2N^2(\alpha_{ee}\alpha_{hh} - \alpha_{eh}^2)]}$$

is the Tellegen chirality parameter. The wavenumbers for the left (+) and right (-) circularly polarized plane waves in chiral medium according to the Maxwell Garnett approach are:

$$\gamma_{MG \pm} = \omega[\sqrt{(\epsilon_{MG}\mu_{MG})} \pm \zeta_{MG}/i]$$

Therefore, the intrinsic impedance

$$\eta_{MG} = \sqrt{(\mu_{MG}/\epsilon_{MG})}$$

of the chiral composite is independent of the wavenumbers. Thus, the Waterman-Truell approach does not account for the electromagnetic parameters of permittivity and permeability and has not included the intrinsic impedance. In order to decrease reflectivity and increase absorptivity, the value of the intrinsic impedance must be known to match the impedance of the surrounding atmosphere.

III. B. 2. Theoretical Models, Formulas and Equations

The generalized Maxwell Garnett model [2] for isotropic chiral composites yields the following for the effective electromagnetic parameters of permittivity, permeability and chirality.

$$\epsilon_{eff} = \epsilon\epsilon_o + \frac{1}{D} (N a_{ee} - N^2 \frac{\Delta}{3\mu\mu_o})$$

$$\mu_{eff} = \mu\mu_o + \frac{1}{D} (N a_{mm} - N^2 \frac{\Delta}{3\epsilon\epsilon_o})$$

$$\kappa_{eff} = \frac{j}{D} N \frac{a_{em}}{\sqrt{\epsilon_o \mu_o}}$$

$$\text{where } D = 1 - N \frac{a_{ee}}{3\epsilon\epsilon_o} - N \frac{a_{mm}}{3\mu\mu_o} + N^2 \frac{\Delta}{9\mu\mu_o \epsilon\epsilon_o} \quad \Delta = a_{ee} a_{mm} - a_{em} a_{me}$$

where ϵ and μ are the relative parameters of the matrix ($\epsilon_r = \epsilon/\epsilon_o$, $\mu_r = \mu/\mu_o$ [1]).

The constitutive relations for the bi-anisotropic chiral media in terms of electric and magnetic flux densities and corresponding dipole moments are expressed in the following equations

$$\mathbf{D} = \boldsymbol{\varepsilon} \cdot \mathbf{E} - i \sqrt{(\boldsymbol{\varepsilon}_0 \mu_0)} \mathbf{K}^T \cdot \mathbf{H}$$

$$\mathbf{B} = \boldsymbol{\mu} \cdot \mathbf{H} + i \sqrt{(\boldsymbol{\varepsilon}_0 \mu_0)} \mathbf{K} \cdot \mathbf{E}$$

and

$$\mathbf{p} = \mathbf{a}_{ec} \cdot \mathbf{E} + \mathbf{a}_{em} \cdot \mathbf{H}$$

$$\mathbf{m} = \mathbf{a}_{mm} \cdot \mathbf{H} - \mathbf{a}_{em} \cdot \mathbf{E}$$

In addition to the above approach, another formula was developed for the design chiral composites. The modified Maxwell Garnett formula for chiral composites, the Chiral Maxwell Garnett Mixing formula [6], describes the macroscopic electromagnetic parameters of permittivity, permeability and chirality with the necessary electric and magnetic polarization terms. The argument begins by stating the material constitutive relations which represent magnetoelectric coupling for the bi-isotropic media

$$\mathbf{D} = \boldsymbol{\varepsilon} \mathbf{E} - i \kappa \sqrt{(\mu_0 \boldsymbol{\varepsilon}_0)} \mathbf{H}$$

$$\mathbf{B} = \boldsymbol{\mu} \mathbf{H} + i \kappa \sqrt{(\mu_0 \boldsymbol{\varepsilon}_0)} \mathbf{E}$$

Where

\mathbf{D} = electric flux

\mathbf{B} = magnetic flux

$\boldsymbol{\varepsilon}$ = permittivity of chiral material

$\boldsymbol{\varepsilon}_0$ = permittivity of the vacuum (or achiral background)

$\boldsymbol{\mu}$ = permeability of chiral material

μ_0 = permeability of the vacuum (or achiral background)

κ = dimensionless parameter of chirality

Thus, the homogeneity of the composite material can be defined by the effective parameters of the mixture. The constitutive equations described by the average flux densities and the associated electric and magnetic fields are:

$$\langle \mathbf{D} \rangle = \boldsymbol{\varepsilon}_{\text{eff}} \mathbf{E} - i \kappa_{\text{eff}} \sqrt{(\mu_0 \boldsymbol{\varepsilon}_0)} \mathbf{H}$$

$$\langle \mathbf{B} \rangle = \boldsymbol{\mu}_{\text{eff}} \mathbf{H} + i \kappa_{\text{eff}} \sqrt{(\mu_0 \boldsymbol{\varepsilon}_0)} \mathbf{E}$$

Including the electric and magnetic polarizability of the constitutive relations yields

$$\langle \mathbf{D} \rangle = \boldsymbol{\varepsilon}_0 \mathbf{E} + \mathbf{P}_e = \boldsymbol{\varepsilon}_0 \mathbf{E} + \mathbf{P}_{ee} + \mathbf{P}_{em}$$

$$\langle \mathbf{B} \rangle = \mu_0 \mathbf{H} + \mathbf{P}_m = \mu_0 \mathbf{H} + \mathbf{P}_{mm} + \mathbf{P}_{me}$$

The definition of the polarizability can be stated as follows:

$$\mathbf{P}_{ij} = n \mathbf{p}_{ij}$$

where i and j are any combination of e and m and let n be the number of spherical chiral scatters per unit volume, whose parameters are ϵ , μ , and κ . Therefore, the dipole moments, p_{ij} , are equal to or directly proportional to the polarizability factor, α_{ij} , and the Lorentzian fields, E_L and H_L , that encompass the surrounding polarization of the field created by the shape of the scatter.

$$\begin{aligned} p_{ee} &= \alpha_{ee} E_L \\ p_{em} &= \alpha_{em} H_L \\ p_{mm} &= \alpha_{mm} H_L \\ p_{me} &= \alpha_{me} E_L \end{aligned}$$

The exciting field for spherical inclusions are defined as:

$$\begin{aligned} E_L &= E + \frac{P_e}{3\epsilon_0} \\ H_L &= H + \frac{P_m}{3\mu_0} \end{aligned}$$

Polarizability factors for single chiral scatters defined in compliance with quasistatic analysis yield

$$\begin{aligned} \alpha_{ee} &= 4\pi a^3 \epsilon_0 \frac{(\mu + 2\mu_0)(\epsilon - \epsilon_0) - \kappa^2 \mu_0 \epsilon_0}{(\mu + 2\mu_0)(\epsilon + 2\epsilon_0) - \kappa^2 \mu_0 \epsilon_0} \\ \alpha_{em} &= 4\pi a^3 \sqrt{(\mu_0 \epsilon_0)} \frac{-j3\kappa\mu_0 \epsilon_0}{(\mu + 2\mu_0)(\epsilon + 2\epsilon_0) - \kappa^2 \mu_0 \epsilon_0} \\ \alpha_{mm} &= 4\pi a^3 \mu_0 \frac{(\mu - \mu_0)(\epsilon + 2\epsilon_0) - \kappa^2 \mu_0 \epsilon_0}{(\mu + 2\mu_0)(\epsilon + 2\epsilon_0) - \kappa^2 \mu_0 \epsilon_0} \\ \alpha_{me} &= 4\pi a^3 \sqrt{(\mu_0 \epsilon_0)} \frac{j3\kappa\mu_0 \epsilon_0}{(\mu + 2\mu_0)(\epsilon + 2\epsilon_0) - \kappa^2 \mu_0 \epsilon_0} \end{aligned}$$

where a is the radius of the sphere with em parameters, permittivity, permeability and chirality. Thus, the effective electromagnetic parameters of the homogeneous chiral slab are:

$$\epsilon_{\text{eff}} = \epsilon_o + 3f\epsilon_o \times \frac{(\epsilon - \epsilon_o)(\mu + 2\mu_o) - f(\mu - \mu_o) - \kappa^2 \mu_o \epsilon_o (1-f)}{[(\mu + 2\mu_o) - f(\mu - \mu_o)][(\epsilon + 2\epsilon_o) - f(\epsilon - \epsilon_o)]} - \kappa^2 \mu_o \epsilon_o (1-f)^2$$

$$\mu_{\text{eff}} = \mu_o + 3f\mu_o \times \frac{(\mu - \mu_o)[(\epsilon + 2\epsilon_o)] - \kappa^2 \mu_o \epsilon_o (1-f)}{[(\mu + 2\mu_o) - f(\mu - \mu_o)][(\epsilon + 2\epsilon_o) - f(\epsilon - \epsilon_o)]} - \kappa^2 \mu_o \epsilon_o (1-f)^2$$

$$\kappa_{\text{eff}} = \frac{9f\kappa\mu_o \epsilon_o}{[(\mu + 2\mu_o) - f(\mu - \mu_o)][(\epsilon + 2\epsilon_o) - f(\epsilon - \epsilon_o)]} - \kappa^2 \mu_o \epsilon_o (1-f)^2$$

where $f = n \cdot 4\pi a^3/3$.

According to reference [5], there are four additional constitutive equations which describe the effective properties of isotropic chiral composites: 1) the Tellegen equations (also used to support the previously cited Maxwell Garnett Approach); 2) the Drude-Born-Fedov equations; 3) the Condon's Time-Harmonic equations; and 4) the Post equations. Assuming the volumetric inclusion portion of the chiral material to be represented by small, mutually noninteracting spheres. Let N be the number of spheres per unit volume. Also assume the composite medium to be a homogeneous, nonvacuous region with polarization and magnetization for the respective polarization and magnetization field approximated as

$$\mathbf{P} = N \mathbf{p}_o, \quad \mathbf{M} = N \mathbf{m}_o.$$

Therefore the \mathbf{D} and \mathbf{B} fields for the effective medium can be written as

$$\mathbf{D} = (\epsilon_o + N a_{ee})\mathbf{E} + i N a_{em} \mathbf{H},$$

$$\mathbf{B} = (\mu_o + N a_{mm})\mathbf{H} - i N a_{em} \mathbf{E}$$

These constitutive equations are applicable to isotropic chiral composites [5].

The Tellegen Constitutive Equations

The Tellegen constitutive relations describe the discrete random composite as an effectively isotropic, reciprocal chiral medium [5].

$$\mathbf{D} = \varepsilon^{(T)} \mathbf{E} + \zeta^{(T)} \mathbf{H}$$

$$\mathbf{B} = \mu^{(T)} \mathbf{H} - \zeta^{(T)} \mathbf{E}$$

Where

$$\varepsilon^{(T)} = \varepsilon_o + N \alpha_{ee} \quad \mu^{(T)} = \mu_o + N \alpha_{mm} \quad \zeta^{(T)} = i N \alpha_{em}$$

The Drude-Born-Fedorov Constitutive Equations

The Drude-Born-Fedorov constitutive equations are yet another representation of the effective parameters of isotropic chiral medium.

$$\mathbf{D} = \varepsilon^{(DBF)} [\mathbf{E} + \beta^{(DBF)} \nabla \times \mathbf{E}]$$

$$\mathbf{B} = \mu^{(DBF)} [\mathbf{H} + \beta^{(DBF)} \nabla \times \mathbf{H}]$$

where

$$\varepsilon^{(DBF)} = (\varepsilon_o + N \alpha_{ee}) - (N \alpha_{em})^2 / (\mu_o + N \alpha_{mm}),$$

$$\mu^{(DBF)} = (\mu_o + N \alpha_{mm}) - (N \alpha_{em})^2 / (\varepsilon_o + N \alpha_{ee}),$$

$$\beta^{(DBF)} = (N \alpha_{em} / \omega) / [(\varepsilon_o + N \alpha_{ee})(\mu_o + N \alpha_{mm}) - (N \alpha_{em})^2]$$

If the small spheres are not chiral, β , $\zeta^{(T)}$ and $\beta^{(DBF)}$ are all equal to zero, then

$$\varepsilon^{(DBF)} = \varepsilon^{(T)} = \varepsilon_o [1 + 4\pi N a^3 (\varepsilon_r - 1) / (\varepsilon_r + 2)]$$

$$\mu^{(DBF)} = \mu^{(T)} = \mu_o [1 + 4\pi N a^3 (\mu_r - 1) / (\mu_r + 2)]$$

and the effective medium is also achiral [5].

The Condon's Time-Harmonic Constitutive Equations [5]

$$\mathbf{D} = \varepsilon^{(C)} \mathbf{E} + i\omega \chi^{(C)} \mathbf{H}$$

$$\mathbf{B} = \mu^{(C)} \mathbf{H} - i\omega \chi^{(C)} \mathbf{E}$$

where

$$\varepsilon^{(C)} = \varepsilon_o + N \alpha_{ee} \quad \mu^{(C)} = \mu_o + N \alpha_{mm} \quad \chi^{(C)} = N \alpha_{em} / \omega$$

The Post's Constitutive Equations [5]

$$\mathbf{D} = \varepsilon^{(P)} \mathbf{E} + i\xi^{(P)} \mathbf{B}$$

$$\mathbf{H} = (1/\mu^{(P)}) \mathbf{B} + i\xi^{(P)} \mathbf{E}$$

where

$$\varepsilon^{(P)} = (\varepsilon_o + N \alpha_{ee}) - (N \alpha_{em})^2 / (\mu_o + N \alpha_{mm}),$$

$$\mu^{(P)} = \mu_o + N \alpha_{mm}$$

$$\xi^{(P)} = N \alpha_{em} / (\mu_o + N \alpha_{mm}).$$

III. B. 3. Strong-Property-Fluctuation Theory (SPFT)

An alternative to the various forms of the pronounced Maxwell Garnett model is Strong-Property-Fluctuation Theory (SPFT). This theory is based on variations of the Maxwell equations and position averaged values of individual particle polarizabilities. (SPFT) has been formulated for homogenizing chiral composites [3]. The argument begins with the Drude-Born-Fedov constitutive relations of a nonhomogeneous chiral medium

$$\mathbf{D}(\mathbf{r}) = \varepsilon(\mathbf{r})[\mathbf{E}(\mathbf{r}) + \beta(\mathbf{r})\nabla \times \mathbf{E}(\mathbf{r})],$$

$$\mathbf{B}(\mathbf{r}) = \mu(\mathbf{r})[\mathbf{H}(\mathbf{r}) + \beta(\mathbf{r})\nabla \times \mathbf{H}(\mathbf{r})],$$

where

$$\begin{array}{l} \varepsilon(\mathbf{r}) = \text{permittivity scalar} \\ \mu(\mathbf{r}) = \text{permeability scalar} \\ \beta(\mathbf{r}) = \text{chirality pseudoscalar} \end{array} \left. \begin{array}{l} \\ \\ \end{array} \right\} \begin{array}{l} \text{All three being implicit functions of} \\ \omega \text{ (circular frequency)} \end{array}$$

Rewritten, the constitutive relations in compact matrix notation are given by:

$$\mathbf{C}(\mathbf{r}) = \mathcal{J} \mathcal{X}(\mathbf{r}) \mathbf{F}(\mathbf{r})$$

with

$$\mathbf{C}(\mathbf{r}) = \begin{pmatrix} \mathbf{D}(\mathbf{r}) \\ \mathbf{B}(\mathbf{r}) \end{pmatrix}, \quad \mathcal{J} = \frac{1}{\omega} \begin{pmatrix} 0 & \mathbf{i} \\ -\mathbf{i} & 0 \end{pmatrix}$$

$$\mathcal{X}(\mathbf{r}) = \gamma+(\mathbf{r}) \gamma-(\mathbf{r}) = \begin{pmatrix} \beta(\mathbf{r}) & \frac{i\omega\mu(\mathbf{r})}{k(\mathbf{r})^2} \\ -\frac{i\omega\varepsilon(\mathbf{r})}{k(\mathbf{r})^2} & \beta(\mathbf{r}) \end{pmatrix}, \quad \mathbf{F}(\mathbf{r}) = \begin{pmatrix} \mathbf{E}(\mathbf{r}) \\ \mathbf{H}(\mathbf{r}) \end{pmatrix}$$

where

$$k(\mathbf{r}) = \omega \sqrt{\epsilon(\mathbf{r}) \mu(\mathbf{r})} \quad \text{and} \quad \gamma^+(\mathbf{r}) = k(\mathbf{r})/[1 - k(\mathbf{r}) \beta(\mathbf{r})]$$

$$\gamma^-(\mathbf{r}) = k(\mathbf{r})/[1 + k(\mathbf{r}) \beta(\mathbf{r})]$$

The goal of this theory was to generalize the strong-permittivity-fluctuation theory of dielectric mixtures to chiral-chiral composites, a composite material in which the particulate, in addition to the matrix media, are chiral. A detailed explanation of this theory can be found in reference [3].

Up to this point, the constitutive relations presented have only applied to variations homogeneous or inhomogeneous forms of isotropic chiral media. The following constitutive relations will form the basis for the behavior of linear polarized waves in anisotropic chiral composites.

III. C. Electromagnetic Fields in a Composite Anisotropic Chiral Medium

A homogeneous composite anisotropic chiral material is described by the following tensor constitutive relations

$$\mathbf{D} = \boldsymbol{\epsilon} \cdot \mathbf{E} + i\xi_c \mathbf{B}$$

$$\mathbf{H} = i\xi_c \mathbf{E} + \boldsymbol{\mu} \cdot \mathbf{B}$$

where

$$\boldsymbol{\epsilon} = \begin{bmatrix} \epsilon & -ig & 0 \\ ig & \epsilon & 0 \\ 0 & 0 & \epsilon_z \end{bmatrix}, \text{ is the permittivity tensor}$$

$$\boldsymbol{\mu} = \begin{bmatrix} \mu & -ik & 0 \\ ik & \mu & 0 \\ 0 & 0 & \mu_z \end{bmatrix}, \text{ is the permeability tensor}$$

and ξ_c is the chirality admittance [20].

Ferrite is any of several magnetic substances that consist essentially of an iron oxide combined with one of more metals (as manganese, nickel, or zinc), have high magnetic permeability and high electrical resistivity. Another proposed form of composite is a combination of chiral and ferrite media.

Constitutive Relations for Nonreciprocal Composite Chiral-Ferrite Media

The constitutive relations for chiral media are [19]

$$\mathbf{D} = \boldsymbol{\epsilon} \mathbf{E} + \boldsymbol{\xi} \mathbf{H},$$

$$\mathbf{B} = \boldsymbol{\mu} \mathbf{H} + \boldsymbol{\zeta} \mathbf{E},$$

$$\begin{aligned}\xi &= \alpha_{cr1} + i\alpha_{ci1} \\ \zeta &= \alpha_{cr2} + i\alpha_{ci2}\end{aligned}$$

where for lossless chiral media

$$\begin{aligned}\alpha_{cr1} &= \alpha_{cr2} = 0 \text{ (for the reciprocal case),} \\ \alpha_{ci1} &= -\alpha_{ci2} \\ \alpha_{cr1} &\neq 0, \quad \alpha_{cr2} \neq 0 \text{ (for the nonreciprocal case),}\end{aligned}$$

The constitutive relations for ferrite media are [19]

$$\begin{aligned}D &= \epsilon E, \\ B &= \mu H,\end{aligned}$$

where

$$\mu = \begin{bmatrix} \mu & ik_m & 0 \\ -ik_m & \mu & 0 \\ 0 & 0 & \mu \end{bmatrix},$$

$\mu = \mu' - \mu''$, $k_m = k_m' - ik_m''$, and the dc magnetic field B_0 is in the z direction. Thus, the composite medium is hypothesized to have the following constitutive relations:

$$\begin{aligned}D &= \epsilon E + \xi H \\ B &= \mu H + \zeta E.\end{aligned}$$

III. D. Wave Propagation and Scattering Characteristics of Chiral Materials

The wave propagation and scattering characteristics of chiral materials differ from those of G/E composites (nonchiral composites) because the conversion of linear polarized waves to alternating elliptical RCP and LCP, right circularly polarized and left circularly polarized fields, respectively. The difference depends on the surface induced current and charge densities at the boundary of chiral materials. The RCP and LCP fields produced by the incident linearly polarized waves, within the spherically shaped chiral inclusion, cause differences in velocity. If multiple interfaces between the chiral inclusion and the achiral matrix are incorporated into the design of the chiral material, multiple scattering occurs due to alternating conversion patterns, i.e. RCP to LCP fields and LCP to RCP fields. Then, as the system experiences multiple scattering, the decrease in the effective transmission of em waves will increase absorption [16].

III. D. 1. The Small Spheres Assumption

The use of spherical geometry when referring to the individual inclusion particles, whether helical or omega (Ω) shaped, is assumed for uniform size distribution. This assumption reduces complications due to inclusion size and shape. Further studies have shown that the absorption patterns due to cross section are larger for spheres than those for spheroids. For this reason, the term chiral sphere is used when addressing the chiral inclusions embedded in an achiral matrix [16].

III. D. 2. Transmission Line Theory For Chiral Composites

Initially, the transmission line theory was used to develop an understanding of how an electromagnetic wave, in the form of a plane wave, propagates through a composite plate composed of a series of uniformly constructed lamina. In this paper, the developed theory was termed, "The Foundational Theory". Assuming the same criteria on a macroscopic basis, a T matrix can be formulated for spherical chiral inclusions embedded within an achiral matrix. The final result of a T matrix, presented below, for a single chiral sphere in nonchiral (or achiral) dielectric medium. The boundary conditions on the electromagnetic fields (E- and H-fields) inside and outside the sphere (assuming continuity at the interfaces) which are expanded through vector spherical functions such as $M(3)$ and $N(3)$, in the T matrix and LCP and RCP fields in a chiral composite (which is analogous to the A_i and B_i coefficients, where $i = 1, 2, 3, \dots, n$ number of lamina or vectors for the filament-current phase correction model) [14],[16].

Thus, the analytical expressions for the effective dielectric constant can be obtained from a software package called MACSYMA. Once the analytic expressions for the lowest order T-matrix elements are known in long-wavelength, results can be used in the Maxwell Garnett and Bruggeman models to calculate initial estimates to the roots of dispersion equations at higher frequencies and concentrations of spherical particles [16].

Scattered Field Coefficients for a Chiral Sphere in a Nonchiral Medium

$$E^s = \sum_n \begin{bmatrix} M^{(3)}_{en} \\ M^{(3)}_{on} \\ N^{(3)}_{en} \\ N^{(3)}_{on} \end{bmatrix} \begin{bmatrix} 0 & (T^{11})_{eon} & 0 & 0 \\ 0 & (T^{11})_{oon} & 0 & 0 \\ 0 & 0 & (T^{22})_{een} & 0 \\ 0 & 0 & (T^{22})_{oen} & 0 \end{bmatrix} \begin{bmatrix} 0 \\ 1 \\ -i \\ 0 \end{bmatrix} \begin{matrix} \\ i^n \frac{(2n+1)}{n(n+1)} \\ \\ \end{matrix}$$

where the elements of the T matrix for a chiral sphere in a dielectric host medium are given by

$$(T^{11})_{oon} = - [W_n(L)A_n(R) + W_n(R)A_n(L)] / [W_n(L)V_n(R) + W_n(R)V_n(L)]$$

$$(T^{22})_{een} = - [B_n(L)V_n(R) + B_n(R)V_n(L)] / [W_n(L)V_n(R) + W_n(R)V_n(L)]$$

$$(T^{11})_{\text{con}} = -[W_n(L)B_n(R) - W_n(R)B_n(L)]/[W_n(L)V_n(R) + W_n(R)V_n(L)]$$

$$(T^{22})_{\text{con}} = -(T^{11})_{\text{con}}$$

where

$$W_n(J) = m\phi_n(mJx)(\zeta_n'(x) - \phi_n'(mJx)\zeta_n(x))$$

$$V_n(J) = \phi_n(mJx)(\zeta_n'(x) - m\phi_n'(mJx)\zeta_n(x))$$

$$A_n(J) = \phi_n(mJx)\phi_n'(x) - m\phi_n'(mJx)\phi_n(x)$$

$$B_n(J) = m\phi_n'(mJx)\phi_n'(x) - \phi_n'(mJx)\phi_n(x)$$

J is either L or R, and x is k'a (where the prime denotes differentiation with respect to the argument). $\phi_n(z) = z j_n(z)$, $\zeta_n(z) = z h_n(z)$, and j_n and h_n are the spherical Bessel and Hankel functions, respectively. The parameters $m_L = k_L/k'$, $m_R = k_R/k'$, and $m = 2m_L m_R / (m_L + m_R)$ [16].

III. D. 4. Propagation in Anisotropic Chiral Medium

The general bianisotropic medium is characterized by the constitutive equations [4]

$$\begin{aligned} D &= \epsilon \bullet E + \xi \bullet H, \\ B &= \mu \bullet H + \zeta \bullet E \end{aligned}$$

Assuming lossless reciprocal medium.

Now, assuming isotropic permittivity and permeability, the constitutive relations for the general anisotropic chiral medium follows

$$\begin{aligned} D &= \epsilon E - j\sqrt{(\epsilon\mu)} \kappa_\phi \bullet H, \\ B &= \mu H + j\sqrt{(\epsilon\mu)} \kappa_\phi \bullet E \end{aligned}$$

the relative chirality κ_ϕ dyadic being real. Consider a special case where a chiral medium is made of metal helices with different handedness aligned with x and y directions. The chirality dyadic can be taken as

$$\kappa_\phi = \kappa_\phi (u_x u_x - u_y u_y).$$

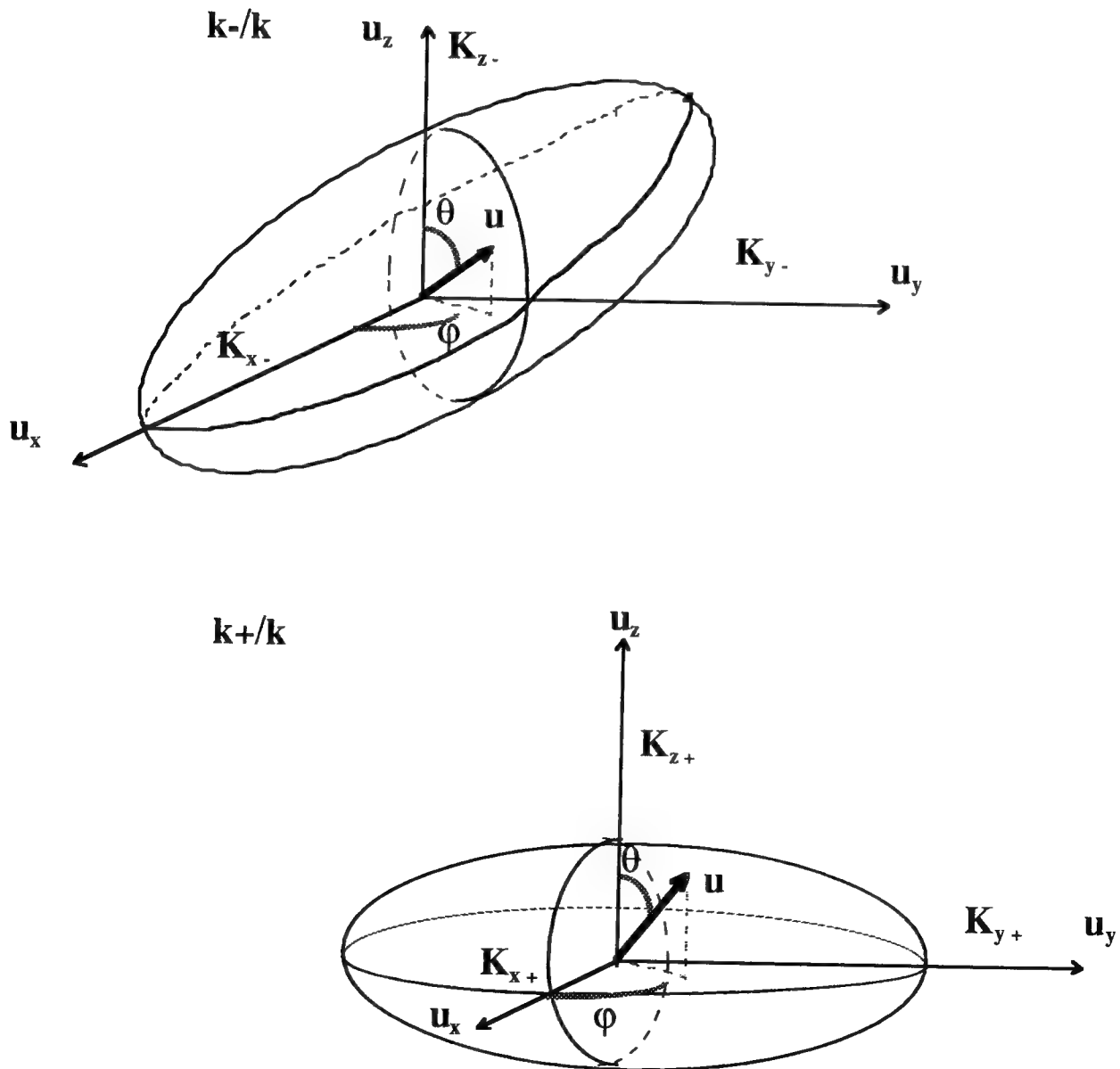
The wave numbers are

$$k_\pm = k \frac{\sqrt{1 - \kappa_\phi^2}}{\sqrt{1 \pm \kappa_\phi \sin^2 \theta \cos 2\phi}}$$

In the present case, there are two planes defined by $\varphi = \pm \pi/4$. The wave numbers for the right-handed and left-handed ellipsoid surfaces illustrated in Figure 1 are $k_-(\theta, \varphi)$ and $k_+(\theta, \varphi)$, respectively. The values of the main axis of the ellipsoids are

$$K_{x\pm} = k \sqrt{\frac{1(-/+)\kappa_\varphi}{1 \pm \kappa_\varphi}}, \quad K_{y\pm} = k \sqrt{\frac{1 \pm \kappa_\varphi}{1(-/+)\kappa_\varphi}}, \quad K_{z\pm} = k \sqrt{1 - \kappa_\varphi}.$$

Figure 1-3. The Elliptic Wave Number Surfaces of $k_-(\theta, \varphi)$ and $k_+(\theta, \varphi)$



III. E. Constitutive Relations for Omega Shaped Inclusions

While advancing the concept of helical shaped inclusions in chiral composites, omega shaped inclusions demonstrated properties which enhanced absorption and/ or reduced reflection from planar lossy slabs. Metal particles shaped like an Ω could reduce the reflection of surfaces when illuminated by linearly polarized and unpolarized electromagnetic waves. The stems of the particles would align with the x-axis with the loop in the (x-y) plane. The medium which consists of these omega particles are termed uniaxial bi-anisotropic, with constitutive relations given by [17]

$$\mathbf{D} = \boldsymbol{\varepsilon} \cdot \mathbf{E} + i K \sqrt{(\boldsymbol{\varepsilon}_o \boldsymbol{\mu}_o)} \mathbf{J} \cdot \mathbf{H}$$

$$\mathbf{B} = \boldsymbol{\mu} \cdot \mathbf{H} + i K \sqrt{(\boldsymbol{\varepsilon}_o \boldsymbol{\mu}_o)} \mathbf{J} \cdot \mathbf{E}$$

Here

The uniaxial dyadics with transverse (t) and normal components (n) are:

$$\boldsymbol{\varepsilon} = \boldsymbol{\varepsilon}_o (\boldsymbol{\varepsilon}_t \mathbf{I}_t + \boldsymbol{\varepsilon}_n z_o z_o)$$

$$\boldsymbol{\mu} = \boldsymbol{\mu}_o (\boldsymbol{\mu}_t \mathbf{I}_t + \boldsymbol{\mu}_n z_o z_o)$$

where z_o stands for the unit vector along the z-axis (normal to the interfaces) and the transverse unit dyadic and the 90° rotator in the (x-y) plane are:

$$\mathbf{I}_t = x_o x_o + y_o y_o \quad \text{and} \quad \mathbf{J} = z_o \times \mathbf{I}_t = y_o x_o - x_o y_o$$

Additional coupling provided by the omega particles is measured by the coupling parameter K , given by the following equation:

$$K = \frac{j}{2} (\boldsymbol{\mu}_t - \boldsymbol{\varepsilon}_t)$$

when the reflection coefficient equals zero. The respective reflection and transmission coefficients for a nonsymmetric slab in air can be found using transmission-line theory and are expressed as the following [17]:

$$R = \frac{(Y_o + Y_-)(Y_o - Y_+)[1 - \exp(-2j\beta d)]}{(Y_o + Y_+)(Y_o + Y_-) - (Y_o - Y_-)(Y_o - Y_+) \exp(-2j\beta d)}$$

$$T = \frac{2(Y_+ + Y_-)Y_o \exp(-j\beta d)}{(Y_o + Y_+)(Y_o + Y_-) - (Y_o - Y_-)(Y_o - Y_+) \exp(-2j\beta d)}$$

where d is the slab thickness and Y_o symbolizes the free space wave admittance.

The polarization of transverse electric and magnetic fields are best characterized by wave impedances or admittances for plane linearly polarized electromagnetic waves propagating in uniaxial Ω media. The admittances for TM- and TE-polarized fields are:

$$Y_{\pm} = \sqrt{\frac{\epsilon_z \epsilon_t}{(\mu_o \mu_t)(1 - \frac{k_t^2}{k_o^2 \epsilon_n \mu_t})}} \frac{1}{L} \times \sqrt{\frac{(1 - \frac{k_t^2}{k_o^2 \epsilon_n \mu_t} - K^2)(-1 \pm j \frac{K}{\sqrt{\epsilon_t \mu_t}})}{\epsilon_t \mu_t}}$$

$$Y_{\pm} = \sqrt{\frac{\epsilon_z \epsilon_t}{(\mu_o \mu_t)L}} \sqrt{\frac{(1 - \frac{k_t^2}{k_o^2 \epsilon_n \mu_t} - K^2)(-1 \pm j \frac{K}{\sqrt{\epsilon_t \mu_t}})}{\epsilon_t \mu_t}}$$

respectively, where the upper sign corresponds to the waves in the positive z-direction and the lower sign to the waves traveling in the negative z-direction. Here k_t is the transverse part of the propagation factor and $k_o = \omega\sqrt{\epsilon_o \mu_o}$.

The propagation factors of the TM- and TE-polarization waves, β , included in the reflection and transmission coefficients are:

$$\beta = \pm \sqrt{\frac{\epsilon_t}{\epsilon_n} (k_o^2 \epsilon_n \mu_t - k_t^2) - k_o^2 K^2} \quad \text{and} \quad \beta = \pm \sqrt{\mu_t (\mu_n (k_o^2 \epsilon_n \mu_t - k_t^2) - k_o^2 K^2)}$$

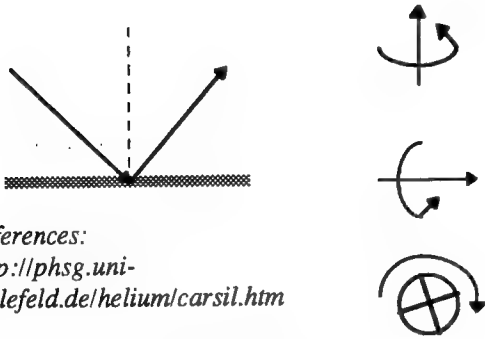
respectively [17].

Therefore, there are three material parameters that control the reflection and transmissions properties of uniaxial omega bianisotropic composite slabs: the dielectric permittivity, magnetic permeability and the coupling parameter. Thus, the adjustment of the magneto-electric interaction, K , the input impedance and the free-space impedance can be matched to achieve low levels of reflection over wide frequency bands [17].

IV. Other Composite Types

IV. A. Quasioptic Composites

The Faraday-Kerr effect is the scientific explanation of how certain material properties change plane polarized light at optical frequencies (Figure 1-4). By using composites made of rare-earth materials and ferrites, similar effects can be simulated at quasioptical frequencies, otherwise known as microwave and millimeter wave frequencies. Such composite types are useful for changing the polarization of incident microwave energy [1].



References:

<http://phsg.uni-bielefeld.de/helium/carsil.htm>

<http://bessrc.msd.anl.gov/11id.htm>

Figure 1-4. The Faraday Effect describes the rotation and the Kerr Effect explains the directionality. However the Kerr Effect can be described by three different subeffects:

- a) Polar effect - Magnetization occurs normal to the surface of reflection.
- b) Longitudinal effect - Magnetization occurs parallel to the surface of reflection.
- c) Transverse effect - Magnetization occurs perpendicular to the plane of incidence.

IV. B. Dielectric Composites

One of the major concerns in the manufacture of composites is low cost, high quality. The design of modern electronic/communication components requires low-loss, high-permittivity dielectrics. For example, consider a two-phase mixture of polystyrene, a high-quality dielectric with low permittivity and a dielectric constant of 2.1; and barium titanate, an expensive high-permittivity material, with a dielectric constant greater than 1,000. With the appropriate volume fractions, the composite formed would possess the low-cost, low-permittivity properties of polystyrene and the high-permittivity properties of barium titanate. Thus, the resulting composite would have high permittivity with respect to polystyrene and low cost with respect to barium titanate [1].

CONCLUSION

In conclusion, graphite/epoxy composites currently make the greatest contribution to industrial and military systems. Chiral composites have the potential to make substantial contributions to future applications due to the additional degree of freedom supplied by the chirality parameter. Finally, quasi-optic and dielectric composites have electromagnetic properties that produce the predictable behavior needed in electromagnetic radio frequency responses. A separate research study is suggested for the latter composites due to their potential economic and structural improvements. Additional research topics include: 1) Techniques used to Measure Parameters of Advanced Composite Materials; and 2) Evaluation of Advanced Composite Materials as a Function of Frequency and Temperature.

APPENDIX A
GEOMETRY OF LAMINATED COMPOSITES
T- AND Π - CIRCUIT SECTIONS
OF
EQUIVALENT-TRANSMISSION-CIRCUIT-LINE MODEL

Figure 1. Geometry of M-ply laminated composites.

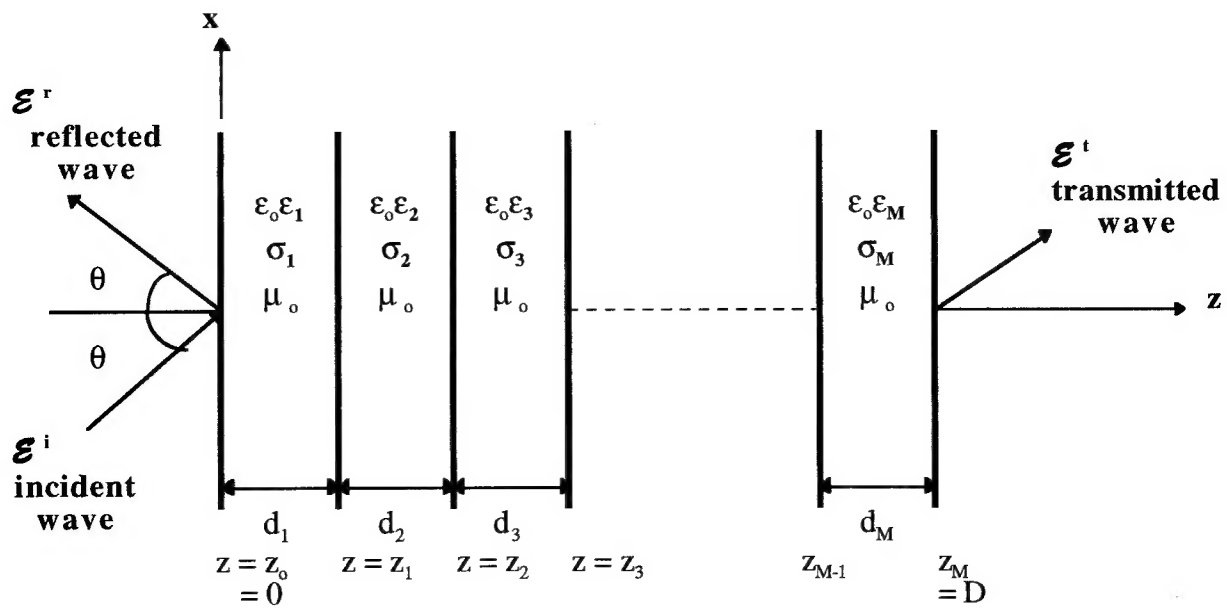
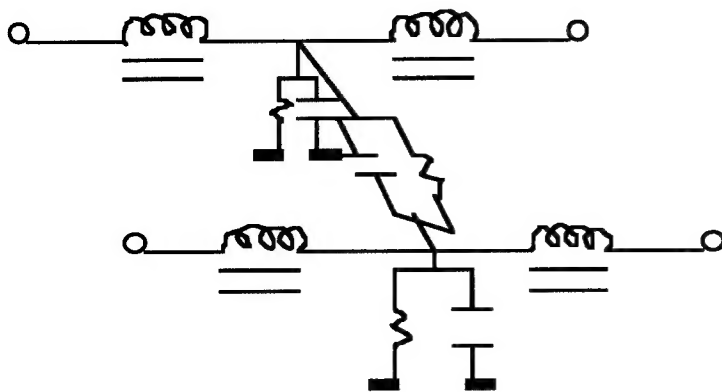
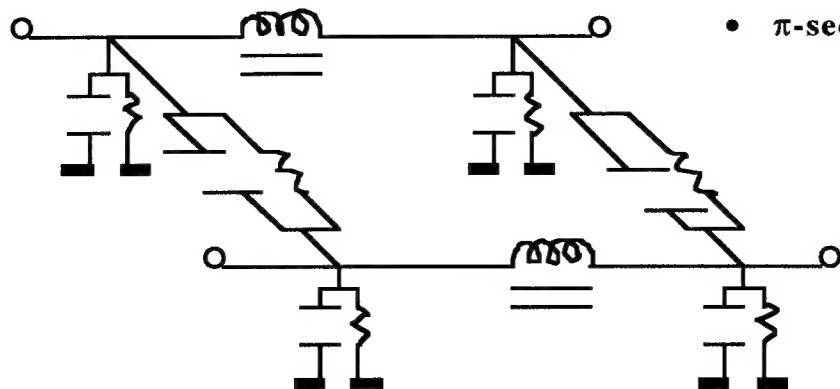


Figure 2. Basic Schematic Diagram of T- and π -sections



• T-section



• π -section

REFERENCES

- [1] P. S. Neelakanta and K. Subramaniam. "Controlling the Properties of Electromagnetic Composites". *Advanced Materials & Processes*. Volume 141, Number 3, March 1992, pp. 20-25.
- [2] C. R. Simovski, A. A. Sochava, and S. A. Tretyakov. "Influence of Chiral Shapes of Individual Inclusions on the Absorption in Chiral Composite Coatings". *Electromagnetics*. Volume 16, Number 2, March-April 1992, pp. 113-127.
- [3] A. Lakhtakia and B. Michel. "Strong-property-fluctuation Theory for Homogenous Chiral Particulate Composites". *Physical Review E*. Volume 51, Number 6, June 1995, pp. 5701-5707.
- [4] I. V. Lindell and A. J. Viitanen. "Plane Wave Propagation in an Anisotropic Chiral Medium with Isotropic Permittivity and Permeability". Helsinki University of Technology, Espoo (Finland), Electromagnetic Laboratory. Report Numbers: ISBN-951-22-1651-5, REPT-152. June 1993, pp. 1-13.
- [5] A. Lakhtakia, V. V. Varadan, and V. K. Varadan. "Dilute Random Distribution of Small Chiral Spheres". *Applied Optics*. Volume 29, Number 25, September 1990, pp. 3627-3632.
- [6] I. V. Lindell and A. H. Sihvola. "Chiral Maxwell-Garnett Mixing Formula". *Electronics Letters*. Volume 26, Number 2, January 1990, pp. 118-119.
- [7] F. Mariotte, and S. A. Tretyakov. "Maxwell Garnett Modeling of Uniaxial Chiral Composites with Bianisotropic Inclusions". *Journal of Electromagnetic Waves & Applications*. Volume 9, Numbers 7/8, 1995, pp. 1011-1025.
- [8] Y. Wenyan, "Electromagnetic Scattering by Some Composite Bianisotropic Eccentric Cylinder". *Microwave and Optical Technology Letters*. Volume 10, Number 3, October 1995, pp. 177-182.
- [9] S. A. Tretyakov, "Electromagnetics of Complex Media: Chiral, Bi-isotropic, and Certain Bianisotropic Materials (A Review)". *Journal of Communications Technology and Electronics*. Volume 39, Number 14, 1994, pp. 32-44.
- [10] M. H. Umari, V. V. Varadan, and V. K. Varadan. "Rotation and Dichroism Associated with Microwave Propagation in Chiral Composite Sample". *Radio Science*. Volume 26, Number 5, September-October 1991, pp. 1327-1334.
- [11] A. Lakhtakia, "Application of the Waterman-Truell approach for Chiral Composites". *International Journal of Electronics*. Volume 75, Number 6, December 1993, pp. 1243-1249.
- [12] D. R. Pflug, "Composite Material Aircraft Electromagnetic Properties and Design Guidelines". Atlantic Research Corporation. Report Number: 50-5779, N00019-79-C-0634. 1981.
- [13] C. Chen, M. Lin. and R. Wu, "Plane-Wave Shielding Characteristics of Anisotropic Laminated Composites". *IEEE Transactions on Electromagnetic Compatibility*. Volume 35, Number 1, February 1993, pp. 21-27.

- [14] C. Chen, and H. Chu. "Shielding and Reflection Properties of Periodic Fiber-Matrix Composite Structures". IEEE Transactions on Electromagnetic Compatibility. Volume 38, Number 1, February 1996, pp. 1-6.
- [15] C. Chen, M. Chiu, and R. Wu. "Time-Domain Analysis of Propagation in Inhomogeneous Anisotropic Lossy Slabs". IEEE Transactions on Antennas and Propagation. Volume 41, Number 10, October 1993, pp.1456-1457.
- [16] Y. Ma, V. V. Varadan, and V. K. Varadan. "Effects of chiral microstructure on em wave propagation in discrete random media". Radio Science. Volume 24, Number 6, November-December 1989, pp. 785-792.
- [17] A. A. Sochava and S. A. Tretyakov. "Proposed composite material for nonreflecting shields and antenna radomes". Electronics Letters. Volume 29, Number 12, June 1993, pp. 1048-1049.
- [18] C. F. Bohren, et. al. "Microwave-absorbing chiral composites: Is chirality essential or accidental?" Applied Optics. Volume 31, Number 30, October 1992, pp. 6403-6407.
- [19] C. M. Krowne, "Electromagnetic properties of nonreciprocal composite chiral-ferrite media". IEEE Transactions on Antennas and Propagation. Volume 41, Number 9, September 1993, pp. 1289-1295.
- [20] Z. X. Shen, "Scattering by a circular impedance cylinder coated with a composite anisotropic chiral sheath". Journal of Electromagnetic Waves and Applications. Volume 8, Number 12, 1994, pp.1625-1644.
- [21] R. Ro, V. K. Varadan, and V. V. Varadan. "Measurement of the electromagnetic properties of chiral composite materials in the 8-40 Ghz range". Radio Science. Volume 29, Number 1, Jan. - Feb. 1994, pp. 9-22.
- [22] F. J. Darnes, J. W. Haffner and E. S. Hughes.: "Advanced composites equipment support module", Prepared by Rockwell International Corporation for Air Force Flight Dynamics Laboratory, Contract No. F33615-77-C-5264, (AFFDL TR 78- 125), 1978, pp. 12, 61-69.
- [23] R. O. Brick, et. al. "Investigation of effects of electromagnetic energy on advanced composite aircraft structures and their associated avionic/electrical Phase II-Volume 1", Report Number: D180-20186-4, Contract Number: N00019-76-C-0497, The Boeing Company, Naval Air Systems Command, September 1977, pp. 20, 40-41, 159.
- [24] M. Lin, et. al. "Transient Propagation in Anisotropic Laminated Composites". IEEE Transactions on Electromagnetic Compatibility. Volume 35, Number 3, August 1993, pp. 357-364.
- [25] Whites, K. W. "Full-Wave Computation of Constitutive Parameters for Lossless Composite Chiral Materials". IEEE Transactions on Antennas and Propagation. Volume 43, Number 4, April 1995, pp. 376-384.
- [26] Dr. D. R. Pflug, Private Consultation, Rome Laboratory, Griffis Air Force Base, Electromagnetic Reliability Science and Technology, 26 Electronic Parkway, Rome, New York 13441, July-August 1996.

***MISSION
OF
ROME LABORATORY***

Mission. The mission of Rome Laboratory is to advance the science and technologies of command, control, communications and intelligence and to transition them into systems to meet customer needs. To achieve this, Rome Lab:

- a. Conducts vigorous research, development and test programs in all applicable technologies;
- b. Transitions technology to current and future systems to improve operational capability, readiness, and supportability;
- c. Provides a full range of technical support to Air Force Materiel Command product centers and other Air Force organizations;
- d. Promotes transfer of technology to the private sector;
- e. Maintains leading edge technological expertise in the areas of surveillance, communications, command and control, intelligence, reliability science, electro-magnetic technology, photonics, signal processing, and computational science.

The thrust areas of technical competence include: Surveillance, Communications, Command and Control, Intelligence, Signal Processing, Computer Science and Technology, Electromagnetic Technology, Photonics and Reliability Sciences.